A STUDY ON KINETICS OF METHANE OXIDATIVE STEAM REFORMING (OSR) OVER Pt-Ni/δ-Al_2O_3 BIMETALLIC CATALYSTS

by

Elif Erdinç

B.S., Chemical Engineering, Boğaziçi University, 2012

Submitted to the Institute for Graduate Studies in
Science and Engineering in partial fulfillment of
the requirements for the degree of
Master of Science

Graduate Program in Chemical Engineering
Boğaziçi University

2014

to my family

ACKNOWLEDGEMENTS

First, I would like to express my truthful gratitude to my thesis supervisor Prof. Ahmet Erhan Aksoylu, who devoted his valuable time to guide, help and motivate me all the time. It was a privilage for me to work with him during my thesis, since he did not hesitate to share his expertise and experiences in catalysis and reaction engineering. I am very grateful to Prof. Aksoylu for his real support in every condition.

I would like to express my sincere appreciations for the members of thesis committee, Assoc. Prof. A. Kerim Avcı and Assoc. Prof. Hasan Bedir, for devoting their valuable time to read and comment on my thesis.

I would like to thank my friends Melek Selcen Başar, Belkız Merve Eropak, Aybüke Leba, Aysun İpek Paksoy, Sezin Sezen, Ali Uzun, and Janset Yener for giving me their everlasting friendship, endless supports and happy moments worth remembering. Their intimate friendship was the most valuable gain of my master years.

I also would like to thank Hazal Bal and Serhat Erşahin for their friendship and support during long days and nights while conducting our experiments. Heartfelt thanks are for Kerem Aksakal, Begüm Alaybeyoğlu, Barış Burnak, Elif Can, Özgür Yaşar Çağlar, Emre Demirel, Coşar Doğa Demirhan, Utku Deniz, Yeşim Düşova, Can Ekici, Çiğdem Ekmen, Pınar Eribol, Özge Ertem, Elif Gençtürk, Büşra Gürses, Didem Büşra Kabakçı, Burcu Karagöz, Hayri Onur Kavaklı, Sinan Koç, Manuchehr Nadjafi, Çağla Odabaşı, and Cansu Yassı for their friendship and giving me endless support, and motivation during my studies.

Special thanks to Feyza Gökaliler and Burcu Selen Çağlayan, who guided me whenever I needed their help.

Cordial thanks for Bilgi Dedeoğlu for his technical assistance and also Melike Gürbüz, Başak Ünen and Yakup Bal for their friendly attitude.

Finally, I would like to express my dearest thanks to my beloved family for their patience, encouragement and moral support throughout my whole life. Their endless love and trust in me was what made me motivated all the time. Especially, love of my precious nephew always made me feel alive. This is why I dedicate this work to them.

The graduate scholarship provided by TÜBİTAK for my M.S. studies deserves thankful recognition.

ABSTRACT

A STUDY ON KINETICS OF METHANE OXIDATIVE STEAM REFORMING (OSR) OVER Pt-Ni/δ-Al_2O_3 BIMETALLIC CATALYSTS

The aim of the current study is to obtain a reliable power law type rate expression for methane OSR over Pt-Ni/δ-Al_2O_3 catalyst valid for practical experimental condition ranges. In this context, 0.2wt.%Pt-10wt.%Ni/δ-Al_2O_3 and 0.3wt.%Pt-10wt.%Ni/δ-Al_2O_3 catalysts were prepared by sequential impregnation method. Methane OSR performance of these catalysts were tested for constant S/C feed ratio at 450 °C. The performance test results showed that increasing residence time and C/O_2 feed ratio decreased OSR activity, whereas increase in temperature led to higher methane conversions. As the effect of Pt:Ni metal loading did not lead to significant changes in activity, the following preliminary kinetic tests were conducted over 0.2Pt-10Ni catalyst to determine kinetically controlled, mass transfer limitations free, experimental conditions. Based on the outcomes of the preliminary test results, the kinetic study was performed at 375 °C with feed ratio regions of $4.0 < C/O_2 < 7.34$ and $2.03 < S/C < 3.08$. 17 pairs of kinetic experiments were conducted by changing partial pressures of reactants, methane, oxygen, and steam, and residence time, W/F. Reaction orders were estimated as 0.81, 1.60 and 0.44 in methane, oxygen and steam, respectively, by using multivariable non-linear optimization function of MATLAB™. The apparent activation energy of methane OSR was calculated as 31.99 kJ mol^{-1} and pre-exponential factor as 0.366 μmol $mgcat^{-1}$ s^{-1} $kPa^{-2.85}$ for the 350-425 °C temperature interval. The same analysis performed for a narrower temperature range, 350-400 °C, i.e. $375^{\pm}$ 25 °C, gave k_0 and E_A values as 0.956 μmol $mgcat^{-1}$ s^{-1} $kPa^{-2.85}$ and 39.05 kJ mol^{-1}, respectively, confirming the high sensitivity of OSR pathway to temperature.

ÖZET

BİMETALİK Pt-Ni/δ-Al_2O_3 KATALİZÖRLERİ ÜZERİNDE METANIN OKSİDATİF BUHAR REFORMLAMASI (OSR) KİNETİK ÇALIŞMASI

Bu çalışmanın amacı, uygun Pt-Ni/Al_2O_3 katalizörü üzerinde metanın oksidatif buhar reformlaması (OSR) için güvenilir bir üssel hız denklemi elde etmektir. Bu bağlamda, ağırlıkça %0.2Pt-%10Ni/δ-Al_2O_3 ve %0.3Pt-%10Ni/δ-Al_2O_3 katalizörleri ardışık emdirilme yöntemiyle hazırlanmıştır. Bu katalizörlerin metan OSR performansları sabit buhar/karbon (S/C) besleme oranında ve 450 °C'de test edilmiştir. Performans test sonuçları, reaktörde kalma süresindeki ve karbon/oksijen (C/O_2) besleme oranlarındaki artışın OSR aktivitesini azalttığını, sıcaklık artışının ise daha yüksek metan dönüşümü sağladığını göstermiştir. Pt:Ni metal yükleme oranı aktivite üzerinde önemli bir etki göstermediğinden, kütle transferi sınırlamaları olmayan kinetik çalışmalar için ön testler 0.2Pt-10Ni katalizörü üzerinde sürdürülmüştür. Ön kinetik testlerin sonuçları doğrultusunda, kinetik çalışmalar 375 °C'de $4.0 < C/O_2 < 7.34$ ve $2.03 < S/C < 3.08$ besleme oranları aralığında yapılmıştır. Reaktanların (metan, oksijen ve buhar) kısmi basınçları ve reaktörde kalma süreleri değiştirilerek 17 çift kinetik deney yapılmıştır. MATLAB^{TM} ortamında çoklu değişkenli doğrusal olmayan fonksiyon kullanılarak, metan, oksijen ve buhar reaksiyon mertebeleri sırasıyla 0.81, 1.60 ve 0.44 olarak belirlenmiştir. Metan OSR reaksiyonunun 350-425 °C sıcaklık aralığındaki görünür aktivasyon enerjisi (E_A) ve frekans faktörü (k_0) sırasıyla 31.99 kJ mol^{-1} ve 0.366 µmol $mgcat^{-1}$ s^{-1} $kPa^{-2.85}$ olarak hesaplanmıştır. Bu sıcaklık aralığı 350-400 °C (375 °C $\pm$ 25 °C) olacak şekilde daraltıldığında ise, E_A ve k_0 değerleri sırasıyla 39.05 kJ mol^{-1} ve 0.956 µmol $mgcat^{-1}$ s^{-1} $kPa^{-2.85}$ olarak hesaplanmıştır; bu sonuçlar OSR mekanizmasının sıcaklığa karşı yüksek hassasiyet gösterdiğini onaylamaktadır.

TABLE OF CONTENTS

LIST OF FIGURES

LIST OF TABLES

LIST OF SYMBOLS

C	Concentration
E_A	Activation energy
F	Flow rate
k_0	Pre-exponential factor
P	Partial pressure
r	Reaction rate
R	Universal gas constant
T	Temperature
W	Catalyst weight
x	Conversion
α	Reaction order of methane
β	Reaction order of oxygen
γ	Reaction order of steam

LIST OF ACRONYMS/ABBREVIATIONS

ATR	Autothermal Reforming
BOS	Birleşik Oksijen Sanayi
DI	Deionized
FC	Fuel Cell
FP	Fuel Processor
GC	Gas Chromatograph
HC	Hydrocarbon
HPLC	High Performance Liquid Chromatography
HTS	High Temperature Shift
LPG	Liquefied Petroleum Gas
LTS	Low Temperature Shift
NG	Natural Gas
OD	Outer Diameter
OSR	Oxidative Steam Reforming
PEMFC	Proton Exchange Membrane Fuel Cell
POX	Partial Oxidation
PrOX	Preferential Oxidation
RWGS	Reverse Water-Gas Shift
SR	Steam Reforming
SS	Stainless Steel
TCD	Thermal Conductivity Detector
TOS	Time-on-Stream
TOX	Total Oxidation
WGS	Water-Gas Shift

1. INTRODUCTION

Continuously increasing worldwide energy requirement causes strong dependence on fossil based energy sources, which creates environmental issues such as air pollution and global warming, and political and economic chaos (Gupta, 2009). Increased awareness about the effects of greenhouse gas emission on climate, and decreasing natural resources per capita have directed researchers to find out the ways of converting fossil fuels to the other forms of fuels which can be used is more efficiently and more environment-friendly ways in energy generation (Tiemersma *et al*., 2012; Li *et al*., 2013).

Fuel cell technology has been an important research area due to higher energy conversion efficiency and lower greenhouse gases emission. Although efficiency of the conversion of methane to electricity in a simple cycled combustion engine is 35-40% due to thermodynamic equilibrium, this value reaches to 55-60% or more in fuel cells. Another advantage of fuel cells is its applicability to existing energy generators to form hybrid systems (Budzianowski, 2010).

The major feedstock for the fuel cells can be methanol, ethanol, natural gas, syngas or hydrogen. The most technologically advanced fuel cell type, especially suitable for small scale operations, is polymer electrolyte membrane fuel cell (PEMFC) and hydrogen is the best fuel because of its high reactivity at its anode. The other advantage of using hydrogen in such systems is low or medium operation temperatures (Rowshanzamir *et al*., 2012).

Hydrogen has become an important fuel and energy carrier because of its advantages in reduction of greenhouse gas emissions, improved energy security, and increased energy efficiency. There are several areas that hydrogen is utilized as a feedstock, such as hydrotreating and hydrocracking processes, synthesis gas applications (ammonia and methanol manufacturing, Fischer-Tropsch synthesis), and manufacture of chemicals having specific end uses (Avcı *et al*., 2001; Lackner *et al*., 2012). However, high pressure storage and distribution infrastructure for hydrogen is limited. Therefore; in the near future, small-scale decentralized, on-site hydrogen generation will be the solution for the hydrogen storage and distribution problem (Hagh, 2004; Simeone *et al*., 2008; Rowshanzamir *et al*., 2012).

A fuel processor (FP) is a catalytic system that produce CO-free hydrogen from a hydrocarbon having a well-established distribution network. In an FP, three reactions, namely reforming, water-gas shift and preferential CO oxidation take place in a serial fashion (Gökaliler *et al.*, 2012). The most common way of hydrogen production is the steam reforming (SR) of light hydrocarbons (C_1–C_3) on nickel based catalyst because of well-understood technology and the simplicity of the construction and operation (Avcı *et al*., 2001). However, since SR reaction is highly endothermic and occurs at around 800 °C; considerable energy and heat transfer area, and catalyst deactivation are major issues. This is not suitable for small scale on-site or onboard applications as energy efficiency and compactness are crucial. The other way of hydrogen generation is partial oxidation (POX) of fuels. Although POX has higher reaction rates than SR, its hydrogen yield per carbon is lower. Besides, POX leads to high coke formation (Simeone *et al*., 2008; Rowshanzamir *et al*., 2012). Oxidative steam reforming (OSR) is a combination of steam reforming and partial oxidation and profitable in terms of economic and technical aspects. Exothermic oxidation and endothermic steam reforming provide energy efficiency which ensures the temperature control and reduction in hot-spot formation; therefore, suppresses the catalyst deactivation due to sintering or coking. OSR reduces coke formation by steam feed and increases hydrogen yield due to SR. Moreover, OSR makes the manipulation of the product content by changing H_2O/O_2 feed ratio possible. This has an importance in the production of syngas for especially large-scale gas-to-liquid (GTL) plants. Additionally, the use of OSR as the reforming reaction is advantageous in fuel processors designed for small scale FP-FC combined units because it has compact size, quick response feature, and inexpensive material requirement (Hagh, 2004; Souza *et al*., 2007; Rowshanzamir *et al*., 2012).

The most attractive resource for hydrogen production is natural gas (or methane) due to its abundance and existing transportation facilities. The use of natural gas is more environmentally benign and cleaner path considering the fact that it can also be produced from renewable resources like biomass (Rowshanzamir *et al*., 2012).

In order to design, construct and control an efficient FP, reliable kinetic expressions must be known for each of its catalytic reactions. Considering its high energy efficiency and relatively low reaction temperatures needed, OSR is the preferred reforming reaction in an FP. In our previous studies, several Pt-Ni/Al_2O_3 catalysts have been designed, prepared and

tested by their propane OSR performance. Reliable kinetic expressions for propane OSR over the Pt-Ni system have been obtained (Gökaliler *et al*., 2012). It has been also confirmed by our group that Pt-Ni system has a fuel flexibility and shows high OSR performance for the feeds having propane, methane and their mixture (Gökaliler, 2012).

In the current study, the aim was to obtain a reliable kinetic expression for methane OSR over Pt-Ni/Al_2O_3 system. In this content, two Pt-Ni catalysts resulted with higher performance determined by Gökaliler with different Pt:Ni loading ratios were prepared. Then, performance tests were conducted over these two catalysts to determine the superior one by changing carbon/oxygen feed ratio, residence time and reaction temperature. In the kinetic tests, methane conversion of the catalyst was determined for various steam/carbon, carbon/oxygen space time and reaction temperature values, which were determined according to the practical reaction conditions over the selected catalyst. Upon the evaluation of the experimental findings, the parameter values of the power-law type kinetics were determined by using non-linear multivariable optimization tool of the MATLAB^{TM} code.

Chapter 2 contains literature survey including information about fuel cells, hydrogen production and fuel processors, and followed by detailed information about FP reactions and advantages of OSR and also active and selective catalysts for this reaction. The experimental systems and procedures used in the present study are presented in Chapter 3. The results obtained in the experiments and related discussions can be found in Chapter 4. Finally, Chapter 5 includes the conclusions attained from the present study and recommendations for future work.

2. LITERATURE SURVEY

2.1. Fuel Cells

A fuel cell (FC) is an electrochemical device that is based on the combination of hydrogen oxidation over one electrode and reduction of oxygen passes over the other one, to produce electricity. In FC operation, water and heat are the by-products. Recently, this technology has become important because of its advantageous aspects such as high efficiency in energy conversion and less/low harmful emissions. For a distributed energy system applications for residences and small businesses, fuel cell based heat and power cogeneration (CHP) utilizing combined fuel processor (FP), that produces hydrogen from a hydrocarbon, and fuel cell (FP-FC) is considered to be qualified as it offers on-site and real time electricity generation with a high efficiency, and utilization of the heat produced during operation of FP-FC for hot water generation and residential heating (Xie *et al*., 2013).

The most promising and technologically advanced type of fuel cells suitable for small scale applications is proton exchange membrane fuel cell (PEMFC). Hydrogen is the best fuel for PEMFC because of its high reactivity at the anode. Hydrogen is ionized to protons and electrons at the anode of the cell. Protons migrate through a membrane to the cathode where the reaction with oxygen to produce water occurs. Another advantage of using hydrogen in such systems is low or medium operation temperatures (Trimm and Önsan, 2001; Rowshanzamir *et al.*, 2012). The other reasons for popularity of hydrogen fueled PEMFC are its compactness, modularity, high power density and fast response (Çağlayan *et al.*, 2005).

Methanol has also been considered as a fuel for fuel cells; however, due to slow kinetics, methanol gives lower conversion and leads to catalyst deactivation. Thus, hydrogen seems to be more promising fuel, but in turn, hydrogen come up with obvious problems of generation, storage and distribution. For storage case, suggestions of use of pressurized vessels or metal hydrides in a vehicle found inefficient because they occupy space, increase weight, and decrease fuel efficiency. For the same issue, carbon nonofibers may be an

alternative, but the production and distribution of the gas is difficult. Ultimately, studies has been focused on the design of on-site hydrogen generation (Trimm and Önsan, 2001).

2.2. Hydrogen

Nowadays although many alternative sustainable energy sources have emerged, the so-called "hydrogen economy" has received particular attention. Hydrogen based energy systems provide viable and advantageous high-quality energy services in a wide range of applications. They are preferable in clean, safe and sustainable energy production. Hydrogen also provides an ideal complement to electricity since both are high quality energy carriers and they both are environmental-friendly. Though storing electricity efficiently is still a technological problem, storing hydrogen for further use is possible (Barreto, 2003; Wang *et al*., 2013).

Pure hydrogen can not be found in nature. However, it can be produced from various fossil and non-fossil resources. Therefore, production pathways can be shaped according to fuel supply and distribution infrastructure at different regions. Today, 96% of hydrogen is produced from fossil fuels in the world through major commercial technologies such as methane steam reforming, oil reforming, and coal gasification. Accordingly, initial phase of a "hydrogen economy" is to produce hydrogen from the current competitive fossil fuels. At a later stage, the production system could evolve toward renewable resources (Barreto *et al*., 2003; Rowshanzamir *et al*., 2012).

2.3. Fuel Processors

The production, storage and distribution problems of hydrogen have led to the development of fuel processors (FP). FP is a compact catalytic system which efficiently convert hydrocarbon fuels to hydrogen. Thus, combined FP-PEMFC system is a promising option for small-scale on-site heat and power generation (Gökaliler *et al*., 2012). In a FP, three catalytic reactions in series run to produce CO-free hydrogen to be fed to a fuel cell, which are reforming reactions (i.e. steam reforming, partial oxidation, oxidative steam reforming), water-gas shift reaction and preferential CO oxidation, respectively. It should be noted that CO concentration at the exit of a FP should be less than 40 ppm not to deactivate

platinum-electro catalyst in PEMFC as its anode catalyst is sensitive to even traces of CO at the low operation temperature of PEMFC (Çağlayan *et al*., 2005; Ahmed *et al*., 2006).

The commercially available or scientifically studied FP prototypes encounter some difficulties in control and structure. The key solution to design an easy-to-operate FP is to implement the most active and selective catalysts for all three reactions. The operation and design parameters of all these three reactions should be optimized and the catalysts used should be designed to have activity for combined reactions, such as reforming and high temperature WGS, enabling a compact, energy efficient system with easier control (Gökaliler *et al*., 2008).

2.3.1. Reforming Reactions

Reforming reaction is a well-established technology in the petrochemical and fertilizer industries producing hydrogen as a raw material in manufacturing ammonia, methanol, and other chemicals (Lee *et al*., 2005). Reforming is a catalytic or non-catalytic reaction in which hydrogen is separated from hydrocarbon fuel via oxidation of fuel. Reforming can be carried out in three modes: steam forming (SR), partial oxidation (POX), and oxidative steam reforming (OSR) (Momirlan and Veziroğlu, 2005).

2.3.1.1. Steam Reforming (SR). Steam reforming is the reaction of a hydrocarbon with steam to give a mixture of carbon monoxide and hydrogen:

$$C_mH_{2n} + mH_2O \leftrightarrow mCO + (m+n)H_2 \qquad \Delta H > 0 \qquad (2.1)$$

$$C_mH_{2n} + 2mH_2O \leftrightarrow mCO_2 + (2m+n)H_2 \qquad \Delta H > 0 \qquad (2.2)$$

Steam reforming of light hydrocarbons (C_1-C_3) on nickel catalysts is the most widely employed and well-known hydrogen production technology owing to its simplicity in construction and operation (Avcı *et al*., 2001). SR is an endothermic reaction and requires elevated temperatures. Though it is reversible when methane is used as the feed, it is almost irreversible for the higher hydrocarbon feeds. The reaction temperature, feed ratio and product distribution is decided according to the type of catalyst and fuel used (Shekhawat *et*

al., 2011). Need of high temperatures may cause coke formation and to avoid that water should be added in sufficient amounts. For very heavy fuels, non-catalytic partial combustion could be a better option when coking becomes a problem (Trimm and Önsan, 2001).

2.3.1.2. Partial and Total Oxidation (POX and TOX). Partial oxidation (Equation 2.3) is the oxidation of a fuel to give CO and H_2 as the final products. This reaction is highly exothermic and uses low O_2/fuel ratio. Once triggered, the reaction occurs fast and irreversible at temperatures around 750 °C at short contact times, in the order of milliseconds, over precious metals on structured supports, such as monoliths and microchannels. Faster kinetic of POX allows the use of smaller reactor compared to those used for SR. However, depending on the nature of the catalyst, the amount of oxidant in the feed and the residence time, POX reaction may turn to total oxidation (Equation 2.4). Products of total oxidation, or in other words complete combustion, reaction are CO_2 and H_2O (Shekhawat *et al*., 2011).

$$C_mH_{2n} + \frac{1}{2}mO_2 \leftrightarrow mCO + nH_2 \qquad \Delta H < 0 \qquad (2.3)$$

$$C_mH_{2n} + \left(m + \frac{1}{2}n\right)O_2 \leftrightarrow mCO_2 + nH_2O \qquad \Delta H < 0 \qquad (2.4)$$

TOX is also used to heat up a system as an alternative to electrical heating because heating with electricity requires significant battery capacity and fuel must be consumed for its generation. Besides, higher heat generation of total oxidation makes it more preferable (Trimm and Önsan, 2001).

2.3.1.3. Oxidative Steam Reforming (OSR). SR process is the common industrial method for hydrogen production, though it is highly endothermic and SR reactors need to possess large heat transfer areas. Therefore, it is not suitable for on-site FP-FC applications due to the need of large reactor size. On the other hand, POX has higher reaction rates but lower hydrogen yield with respect to SR. Besides, POX tends to coke formation which deactivates catalyst (Rowshanzamir *et al*., 2012).

Oxidative steam reforming (OSR) is a combination of steam reforming and partial/total oxidation, and profitable in terms of economic and technical aspects. Combining exothermic oxidation and endothermic steam reforming provide energy efficiency which ensures the temperature control and reduction in hot-spot formation; therefore, suppresses the catalyst deactivation due to sintering or coking. OSR reduces coke formation and increases hydrogen yield. The special case of OSR is named as autothermal steam reforming (ATR) when zero heat requirement is attained. In OSR, changing the hydrogen concentration and H_2/CO ratio in the product stream can be manipulated through changing the H_2O/O_2 feeding ratio. This is significant in the production of syngas for especially large-scale gas-to-liquid (GTL) plants. Additionally, OSR reactors are advantageous in terms of design as they have compact size, quick response feature, and inexpensive material requirement (Cai *et al*., 2008; Hagh, 2004; Souza *et al*., 2007; Rowshanzamir *et al*., 2012).

2.3.2. Water-Gas Shift (WGS) Reaction

In a fuel processor, the product of the reforming unit, which has CO content between 5-10%, is sent to the following WGS unit, which decreases CO concentration down to 1-1.5%. In this reaction, CO reacts with water to produce H_2 and CO_2 (Equation 2.5) (Natesakhawat *et al*., 2006). WGS is a pressure independent, and slightly exothermic reaction, and it is thermodynamically favored at low temperatures (Lee and Chu, 2003).

$$CO + H_2O \leftrightarrow CO_2 + H_2 \qquad \Delta H = -41.2\ kJ/mol \qquad (2.5)$$

There has been an increasing interest in WGS in the last years owing to its use in applications of combined FP-PEMFC systems. WGS reaction not only decreases CO concentration, but it also increases H_2 amount at the same time. Industrial applications of WGS is in two-stages, high temperature shift (HTS) followed by low temperature shift (LTS). HTS reduces CO concentration from 6-10% to 2-3% at around 300-400 °C using Fe-Cr oxide catalysts and LTS further reduces CO concentration to about 1% or less at around 200-250 °C over commercial $Cu/ZnO/Al_2O_3$ catalyst. Recently, Au based catalyst found to be very active even at low temperatures (Lee and Chu, 2003; Natesakhawat *et al*., 2006; Leppelt *et al*., 2006).

2.3.3. Preferential Oxidation of Carbon Monoxide (PrOX)

An effluent stream of WGS reactor still contains about 1-1.5% CO, which is too high for the low temperature PEMFC. Therefore, a preferential oxidation (PrOX) reactor, which follows the WGS reactor in a fuel processor, is used to decrease the CO concentration in the FP product sent to PEMFC to 40 ppm or less. However, hydrogen oxidation (Equation 2.7) competes with CO oxidation (Equation 2.6), which is not desired as it reduces H_2 yield (Trimm and Önsan, 2001; Lee and Chu, 2003).

$$CO + \frac{1}{2}O_2 \leftrightarrow CO_2 \qquad \Delta H = -283\ kJ/mol \tag{2.6}$$

$$H_2 + \frac{1}{2}O_2 \leftrightarrow H_2O \qquad \Delta H = -242\ kJ/mol \tag{2.7}$$

These reactions are highly exothermic; therefore, proper heat removal is important. In order to reduce CO concentration and to minimize hydrogen oxidation, highly selective catalyst should be preferred. The most successful performance, almost 100% CO conversion, is achieved for low temperature PrOX at 100-150 °C over catalysts containing precious metals Pt or Ir. Additionally, ceria is the best support for this reaction thanks to its high O_2 mobility (Lee and Chu, 2003; Marino *et al*., 2004; Shekhawat *et al*., 2011).

2.3.4. Contributing Reactions

The OSR reaction is complicated and not direct like SR or POX. As an inevitable result of co-feeding oxygen, steam and hydrocarbon; many side reactions occur and these reactions have their own kinetic dependence on reaction temperature, feed composition, type of catalyst and support. Hence, OSR can be written as the net sum of all these reactions occurring at different levels (Shekhawat *et al*., 2006).

The desired reactions produce H_2, CO and heat, and they are SR (Equations 2.1 and 2.2), POX (Equation 2.3), TOX (Equation 2.4), WGS (Equation 2.5), incomplete oxidation (Equations 2.8 and 2.9), and dry reforming (Equation 2.10). On the other hand, some reactions reduce H_2 selectivity. The undesired side reactions which decrease H_2 selectivity

are mainly hydrogen oxidation (Equation 2.11), methanation (Equations 2.12 and 2.13) and reverse water-gas shift reaction (Equation 2.14). Harsh reaction conditions may cause coke formation via hydrocarbon decomposition (Equation 2.15) or Boudouard reactions (Equation 2.16) (Shekhawat *et al*., 2006).

$$C_mH_{2n} + \frac{1}{2}(m+n)O_2 \rightarrow mCO + nH_2O \quad (2.8)$$

$$C_mH_{2n} + mO_2 \rightarrow mCO_2 + nH_2 \quad (2.9)$$

$$C_mH_{2n} + mCO_2 \leftrightarrow 2mCO + nH_2 \quad (2.10)$$

$$H_2 + \frac{1}{2}O_2 \leftrightarrow H_2O \quad (2.11)$$

$$CO + 3H_2 \leftrightarrow CH_4 + H_2O \quad (2.12)$$

$$CO_2 + 4H_2 \leftrightarrow CH_4 + 2H_2O \quad (2.13)$$

$$CO_2 + H_2 \leftrightarrow CO + H_2O \quad (2.14)$$

$$C_mH_{2n} \leftrightarrow mC + nH_2 \quad (2.15)$$

$$2CO \leftrightarrow CO_2 + C \quad (2.16)$$

2.4. Methane as the Hydrocarbon Fuel

The biggest challenge in hydrogen production is to find the suitable technologies for satisfying the demand through economically feasible and environmentally benign ways. Hydrogen can be produced by reforming a variety of readily available hydrocarbons, such

as methanol, ethanol, natural gas, gasoline, and diesel and jet fuels. The most attractive resource for hydrogen production is natural gas, which has methane as its main component, due to its abundance and existing transportation and distribution network. The use of natural gas as the hydrocarbon feed in hydrogen production is more environmentally benign and cleaner path considering the fact that it can also be produced from renewable resources like biomass (Rowshanzamir *et al*., 2012; Malaibari *et al*., 2014). Compared with fossil fuels, water, biomass, etc., natural gas is one of the cheapest options for hydrogen generation (Cai *et al.*, 2008b; Dantas *et al.*, 2012)**.**

Since hydrogen does not exist in pure form in nature and it is not safe and economical to store hydrogen at high pressure, today on-site hydrogen production applications are more attractive for research and technology development. It is confirmed that a fuel processor based on ATR of methane is more suitable for fuel cell stationary and mobile applications because of its low cost, compactness, fast start-up and capability to adapt load variations (Souza and Schmal, 2005; Rowshanzamir *et al*., 2012).

2.5. OSR Catalysts

In the catalyst design, different supports, active metals and promoters are considered. Experimental conditions such as temperature, pressure and feed composition play primary role in obtaining desired product specifications. Almost all performance works for prepared catalysts include such trials to figure out optimum conditions yielding best results.

In OSR, many reactions occur simultaneously or consecutively; therefore, changing feed composition results in different product distributions. Souza and Schmal (2005) have made their study over $Pt/ZrO_2/Al_2O_3$ catalyst. They determined the reaction mechanism as partial oxidation followed by energetically favored steam and dry reforming. They wanted to obtain synthesis gas (syngas) within a certain limit of H_2/CO ratio. Optimal GTL process value of H_2/CO as 2 was achieved for O_2/CH_4 feed ratio equals to 1.0. As O_2/CH_4 ratio was increased, both methane conversion and stability increased due to suppressed coke-based deactivation. However, increase in O_2 feed concentration caused decrease in H_2 and CH_4 yield due to accelerated partial oxidation.

A similar study has been conducted to maximize hydrogen yield by Souza *et al*. in 2010. The catalyst was 5.75 wt.% Ni on γ-Al_2O_3. When they worked in a fixed bed reactor at 750-850 °C and 1.00 bar, they obtained methane conversion around 40-65%, hydrogen yield of 78-84%, carbon monoxide yield of 3-14%, and carbon dioxide yield of 5-18%. Product stream with high H_2 to CO ratio could be achieved, and, low coking and high hydrogen selectivity (81%) were observed in runs with excess steam.

Ruiz *et al.* (2008) has worked on the performance of Pt/$CeZrO_2$ in ATR of methane. The effects of the calcination temperature of the support, reaction temperature, CO_2 existence in the feed, and H_2O/CH_4 feed ratio were studied. For all catalysts, TPSR analyses were made and two-step (indirect) mechanism, the total combustion of methane followed by the steam and dry reforming of methane, was confirmed. The Pt/$Ce_{0.75}Zr_{0.25}O_2$ catalyst showed better activity and stability due to high O_2 vacancies on the support. This explained the use of O_2 in the continuous removal of carbonaceous deposits from the active sites. Water also participated in this mechanism as a carbon carrier from active metal-support interfacial perimeter. They found out that increase in H_2O/CH_4 molar ratio increased CH_4 conversion and H_2/CO molar ratio in the product whereas reaction temperature had an opposite effect. Although the addition of CO_2 to feed stream increased initial methane conversion, it decreased the stability of catalyst.

Performance of a catalyst is affected by the choice of support to a large extent. In literature, there are many works investigating the effect of support on activity, stability, durability and hydrogen selectivity. Cai *et al.* (2008) have studied performance of nickel catalyst on Al_2O_3, ZrO_2-Al_2O_3, CeO_2-Al_2O_3 and ZrO_2-CeO_2-Al_2O_3 supports. The catalysts were prepared by co-precipitation method. The best results for methane conversion, and H_2/CO and H_2/CO_x product ratios were obtained over Ni/ZrO_2-CeO_2-Al_2O_3 catalyst. TPR, XRD and XPS results have proved that formation of ZrO_2-CeO_2 solution provided better dispersion for NiO and blocked $NiAl_2O_4$ formation, and consequently was increased the activity. This catalyst also showed good stability in a 72 h time-on-stream (TOS) test with 0.08%/h deactivation rate.

Nickel catalysts supported on Al_2O_3, CeO_2/Al_2O_3, $Ce_{0.5}Zr_{0.5}O_2/Al_2O_3$, and $Ce_{0.5}Zr_{0.5}O_2$ supports were investigated for their OSR of methane activity by Dantas *et al.* (2012).

Alumina containing supports had higher surface area and better Ni dispersion which were confirmed by BET and XRD, respectively. Similar to Cai *et al.* (2008), they observed ceria-zirconia solution formation which is proposed to be beneficial for the OSR performance. Additionally, they showed that addition of ceria and ceria-zirconia solution to alumina support increased oxygen storage capacity. Another important result that they obtained via Temperature Programmed Reduction and Diffuse Reflectance Spectroscopy is that the supports containing alumina showed higher metal-support interaction.

Escritori *et al.* (2009) were tested nickel catalysts supported on $Ce_{0.5}Zr_{0.5}O_2$, CeO_2/Al_2O_3, $Ce_{0.5}Zr_{0.5}O_2/Al_2O_3$, and Al_2O_3 in autothermal reforming of methane. Sample characterizations were done by BET, X-ray diffraction, H_2 temperature programmed reduction and temperature programmed desorption of CO_2. Nickel dispersion was evaluated using a model reaction, cyclohexane dehydrogenation. Light-off experiments showed that methane autothermal reforming occurs in two steps, by an indirect mechanism in which total combustion at lower temperatures is followed by dry or steam reforming of methane at higher temperatures. Most catalysts exhibited good activity, stability, and gave a H_2/CO product ratio around 2.7 during stability tests lasted 24 h TOS. The best activity was obtained over 10% $Ni/Ce_{0.5}Zr_{0.5}O_2/Al_2O_3$ catalyst and its performance could be explained by its higher reducibility and Ni dispersion.

In a new manner, Gao *et al.* (2008) have tried addition of silica into ceria and zirconia support for nickel-based catalyst. Support was prepared by impregnation of certain amounts of ceria nitrate and zirconia nitrate into silica. They observed that combined support integrated the advantages of SiO_2 and CeO_2-ZrO_2. Catalyst prepared on the combined support has had higher surface area, stronger acidity, better Ni dispersion, better reducibility, higher CO_2 adsorption capacity, and higher methane OSR activity.

Various solid solutions of zirconia were prepared by the glycothermal method with the addition of changing amounts of ceria and calcium oxide was used as a support for Ni catalysts over which partial oxidation and oxidative steam reforming of methane tests were conducted (Takeguchi *et al.,* 2003). In partial oxidation tests, Ni/CaO-ZrO_2 has showed higher activity due to increased reduction rate of NiO and decreased coking. On the other

hand, for oxidative reforming runs, $CaO\text{-}CeO_2\text{-}ZrO_2$ solid solution support was found as a better option in terms of activity and stability due to its higher metal-support interaction.

Razaei *et al.* (2011) and Mosayebi *et al.* (2012) have used nanocrystalline supported nickel catalysts. In their studies, high surface area MgO and $MgAl_2O_4$ supports, respectively, were used as nickel carriers owing to the advantages of surfactant-assisted impregnation method. Both supports have increased methane OSR activity and yielded high catalyst stability.

Nurunnabi *et al.* (2005) have published their results on oxidative steam reforming of methane. In their work, the effect of the addition of noble metal Pt, and the formation and the use of solid solution as a support on OSR performance were studied for Pt/NiO-MgO catalysts. Activity order for the catalysts was determined as Pt/NiO-MgO >> Pt/MgO > NiO-MgO which shows that addition of metal is much more effective than change in the support.

In the metal selection for methane OSR catalysts, activities of metals are thought to similar to those observed in SR (Gökaliler, 2012). In 2003, Ayabe *et al.* determined the metal activity series of the alumina supported catalysts as Rh > Pd > Ni > Pt > Co. As can be seen from that study, although nickel is not the most active metal, the development of nickel-based catalysts for OSR has been the focus of many studies due to the availability and low price of nickel (Dias and Assaf, 2008).

Effect of active metal on the activities of propane and methane OSR catalysts was studied by Ayabe *et al.* in 2003. They tested Co, Ni, Pd, Pt, and Rh on alumina support with 10 wt.% loading for Ni and 2 wt.% for the others. Activity for these metals was determined with the following sequence: Rh > Pd > Ni > Pt > Co. They have stated that nickel catalyst was deactivated due to partial oxidation of Ni at low temperatures. Additionally, although coke deposition was not problematic for methane feed, it was for propane oxidative steam reforming even for high steam feed conditions.

Nurunnabi *et al.* (2006) have studied small amounts of noble metals (Pd, Pt, Rh) addition on NiO-MgO support. They made a comparison between OSR performance of these catalyst with that of only MgO support and commercial Ni catalyst on alumina support, and

proved that their proposed catalyst shows higher activity in oxidative steam reforming of methane. Rh has been determined as the best active metal in terms of OSR activity and coking inhibition. Same researchers have claimed positive effect of small amount of noble metal addition on the methane conversion, especially at low contact time, and resistance to coking because of synergetic mechanism of noble metal and NiO-MgO support.

When cost of the catalyst is considered, nickel based catalysts should have been developed. Additive effect of small amount of noble metals (Pd, Pt, Au, Ir, Rh and Ru) on Ni/α-Al_2O_3 catalyst for oxidative steam reforming of methane reaction has investigated by Yoshida *et al.* (2009). Bimetallic catalysts were prepared by co-impregnation method and catalytic performance and the changes in catalyst bed temperature during reaction were investigated. They have showed that addition of a small amount of noble metals suppressed the formation of hot-spots. They also observed higher catalytic activity over bimetallic catalysts (Pd+Ni, Pt+Ni, Ir+Ni) than monometallic ones (Pd, Pt, Ir).

Mukainakano *et al.* (2007) have investigated bimetallic catalysts, namely Pd-Ni and Rh-Ni in oxidative steam reforming of methane. Bimetallic catalysts were prepared by both co-impregnation and sequential impregnation methods to see the effects of catalyst preparation technique on OSR performance. Bimetallic catalyst had high methane conversions even at low contact times. According to thermographical observations, catalyst preparation method showed a high influence on the reactor bed temperature. Catalyst prepared by sequential impregnation exhibited better resistance to hot-spot formation. Especially Pd-Ni catalyst gave good results probably because of synergetic interaction between Pd and Ni. Surface modifications were analyzed through Extended X-ray Absorption Fine Structure (EXAFS), and the results explained the increase in OSR performance through Pd-Ni interaction.

Dantas *et al.* (2010) have studied the effect of Ag, Fe, Pt and Pd promoters on hydrogen production performance of Ni/$CeZrO_2$ catalyst in methane OSR. Support with Ce/Zr ratio of 1 was prepared by co-precipitation method. Similar to work of Mukainakano *et al.* (2007), both co-impregnation and sequential impregnation were used for metal doping. Monometallic Ni catalyst showed hysteresis with increasing temperature due to existence of oxygenation. Hysteresis effect was disappeared when Pt was added. Prevention of Ni

oxidation at high temperatures was more explicit in the runs conducted over the sample prepared by sequential impregnation (Pt/Ni) than that prepared with co-impregnation (Pt+Ni). As characterization results indicated, Pt-Ni alloys could preferentially be formed on the surface for Pt/Ni catalysts which prevents Ni oxidation. Additionally, Pt-Ni species located in the bed inlet could provide decrease in the bed temperature and temperature gradient compared to the results obtained from the tests conducted over monometallic Ni catalysts.

Hysteresis effect of monometallic Ni catalysts with changing temperature has studied by Li *et al.* (2007). They proved that this effect could be removed by addition of Pt metal to the catalyst. Similar to Mukainakano *et al.* (2007) and Dantas *et al.* (2010), they confirmed that sequential impregnation yields better results than co-impregnation due to Pt-Ni alloy formation near the surface of the catalysts prepared by sequential impregnation. They claimed that changes in the surface caused the decrease in oxidation rate of the species, the increase in reduction rate and, consequently, enables better temperature control of the catalyst bed.

Research group of Yoshida (Mukainakano *et al.*, 2008a) has studied the catalytic performance of monometallic Ni and Pt and two Pt–Ni bimetallic catalysts in steam reforming and oxidative steam reforming of methane. Similarly, hysteresis effect was clearly observed on a Pt–Ni bimetallic catalyst prepared by co-impregnation method and the Ni catalyst for both reactions. In contrast, no hysteresis was observed for a Pt–Ni catalyst that was prepared by sequential impregnation method. These results were justified via characterization results obtained from EXAFS analysis and FTIR-DRIFT studies where CO used as a probe adsorbent. Pt-Ni alloy was found formed on Pt–Ni catalyst prepared by sequential impregnation. On the sample prepared by sequential impregnation, Pt atoms are segregated on the surface enhancing the reducibility of Ni drastically.

Same group has made similar study on the methane OSR performance of Pd–Ni bimetallic catalysts prepared by co-impregnation and sequential impregnation methods. Sequential impregnation was found more effective in suppressing hot spot formation. According to the structural analysis by in situ quick-scanning X-ray absorption fine structure (QXAFS) during the temperature programmed reduction, the sequential impregnation

method led to a higher Pd surface concentration on the bimetallic particles formed with due to the low possibility of the Pd–Ni bond formation. Higher surface concentration of Pd leading higher reducibility of Pd-Ni catalysts than that of monometallic Ni is directly related with the suppression of the hot spot formation (Mukainakano *et al.*, 2008b).

Another study has been conducted to see the effects of addition of promoters on ATR of methane activity of Ni-based catalysts (Dias and Assaf, 2008). They investigated the effect of introducing small amounts of Pt, Pd and Ir (<0.3% by weight) onto Ni/γ-Al_2O_3 catalysts (15% Ni w/w). The results show that promoters neither catalyze partial oxidation, nor cause electronic modifications of nickel sites. On the other hand, addition of small amount of noble metal increased methane ATR conversion through increasing metal surface area and the process is proposed to be independent of type of noble metal added (Dias, 2004). Differences in the catalyst activities were tried to be explained in their further studies. They have focused on the changes in activity, reducibility, capacity of repeated ignition and temperature profile of the reactor resulted from adding small amounts of Pd to Ni/γ-Al_2O_3 methane ATR catalysts. They observed a flatter temperature profile through the catalytic bed due to increased metal surface area. Moreover, use of different Pd sources affected the reducibility of catalysts (Dias and Assaf, 2008).

In our group, OSR of propane was studied over Pt–Ni/δ-Al_2O_3 bimetallic catalysts. In the tests, metal loadings, Ni:Pt loading ratio, and temperature were used as the experimental parameters. In order to investigate the effect of Au existence on the performance of the catalyst, a trimetallic Pt–Ni–Au/δ-Al_2O_3 catalyst was also prepared. Hydrogen production and H_2/CO product ratio was found dependent on Pt-Ni loadings and especially on C/O_2 feed ratio, which was changed between 1.50-2.70. The best hydrogen yield and selectivity were achieved for the highest C/O_2 ratio. An optimum Ni:Pt weight ratio was found around 50, which led to suppressed methanation and enhanced hydrogen production activities. Addition of Au to bimetallic catalyst did not improve activity and selectivity (Gökaliler *et al*., 2008). A kinetic study on OSR of propane was conducted on the best performing catalyst, 0.2Pt10Ni/ δ-Al_2O_3; the results will be presented in detailed fashion in Section 2.6 (Gökaliler *et al.*, 2012).

2.6. OSR Kinetics

There are several studies on kinetics of reforming reactions over various catalysts for different hydrocarbon feeds. In those studies, hydrocarbon source changes from methane to diesel, and choice of catalyst is generally commercial Ni based catalysts, alumina supported Ru, Pt, Ni, Rh, and catalysts prepared on ceria or perovskite structures (Gökaliler *et al*., 2012).

In OSR, there are several reactions occurring simultaneously; among those SR, TOX and WGS are dominant ones and called primary reactions while other reactions, such as methanation, Boudouard reaction, dry reforming etc. are called side/secondary reactions and are ignored in modeling of OSR kinetics for simplification (Gökaliler, 2012). There are two important kinetic studies investigating of mechanism of methane OSR through individual primary reactions involve in OSR. These are the kinetics of partial oxidation by Ma *et al.* (1996) and steam reforming of methane by Xu and Froment (1989). These works are especially useful in modeling methane OSR.

Ma *et al.* (1996) have studied the kinetics of total oxidation of methane, ethane and propane over $Pt/\delta\text{-}Al_2O_3$ catalyst. Oxidation of methane was conducted in a tubular reactor at temperatures between 360-460 °C. They carried out the experiments such as to keep conversion less than 10%. Approximately first order dependence of hydrocarbon and a negative order for oxygen were determined for the power law rate expression. They have mentioned that the best way to describe oxidation of methane is to use a Langmuir-Hinshelwood model in which the surface reaction is between the adsorbed hydrocarbon and adsorbed atomic oxygen.

Intrinsic rate equations for methane steam reforming, methanation and water-gas shift reactions over nickel based catalyst were studied by Xu and Froment (1989). Experimental studies were conducted at temperatures between 500-575 °C. Kinetic study was performed after 70 hours in order to guarantee that catalyst deactivation stemming from sintering is stabilized. They have predicted comprehensive reaction mechanisms and they have come up with a reasonable Langmuir-Hinshelwood type rate expression by taking thermodynamic considerations and statistical significance into account. They concluded that the steam

reforming and water-gas shift reactions run parallel or more or less consecutive to the total combustion, depending on the degree of reduction of the catalyst, which was manipulated by temperature and gas phase composition changes.

Although power-law type of rate expression does not give a detailed idea about mechanisms of reactions, they are beneficial for prediction of system performance, comparison of different catalysts and designing reactors (Hla *et al*., 2011). As far as we know, there are only two OSR kinetic study which yielded power-law type rate expressions (Shekhawat *et al.*, 2006; Gökaliler *et al*., 2012).

Berry *et al.* has studied OSR kinetics using diesel as a hydrocarbon source on Pt, Pd and Ru catalysts supported on alumina. They determined that diesel consumption rate has positive and negative dependencies on diesel and steam partial pressures, respectively. On the other hand, oxygen was classified as being non-monotonic (Shekhawat *et al*., 2006).

The other kinetic study has performed by Gökaliler *et al.* (2012) in which they obtained an easy-to-implement power-law type rate equation for ATR of propane on 0.2wt%Pt-10wt%Ni/δ-Al_2O_3 catalyst at 400 °C steam-to-carbon feeding ratio range of 2.0-3.0 and carbon-to-oxygen feeding ratio range of 3.0-5.4. Orders of reaction were determined as 1.64, 2.44 and -0.59 in propane, oxygen and steam partial pressures, respectively, and the apparent activation energy for propane ATR is calculated as 46.19 ± 4.27 kJ mol^{-1} for the 380-420 °C interval.

3. EXPERIMENTAL WORK

3.1. Materials

3.1.1. Chemicals

The chemicals used for catalyst preparation are presented in Table 3.1. All the chemicals used are research grade with high purity.

Table 3.1. Chemicals used for catalyst preparation.

Chemicals	**Formula**	**Specification (%)**	**Source**	**Molecular Weight (g/mol)**
Aluminum Oxide	γ-Al_2O_3	99.98	Alfa Aesar	101.96
Nickel(II) nitrate hexahydrate	$Ni(NO_3)_2$.6H2O	99	Merck	290.81
Tetraammineplatinum (II) nitrate	$Pt(NH_3)_4(NO_3)_2$	99.995+	Aldrich	387.22

3.1.2. Gases and Liquids

All of the gases used in this study were bought from Birleşik Oksijen Sanayi (BOS) A.Ş. and Linde Group, Istanbul. Table 3.2 and Table 3.3 show the specifications and applications of the liquids and gases employed in this research.

Table 3.2. Specifications and applications of the gases used.

Gas	Specification (%)	Application
Argon	99.995	GC Carrier Gas
Carbon dioxide	99.995	Product
Carbon monoxide	99.999	Product
Dry Air	99.998	GC 6-way Pneumatic Valve
Helium	99.999	GC Carrier Gas
Hydrogen	99.995	Product, Reducing Agent
Methane	99.995	Reactant
Nitrogen	99.998	Inert
Oxygen	99.998	Reactant

Table 3.3. Specifications and applications of the liquids used.

Liquid	Specification	Application
Water	Deionized (DI)	Aqueous solutions, Reactant

3.2. Experimental Systems

The experimental systems used in this study can be divided mainly into three groups:

- Catalyst Preparation Systems: This systems include setups for support preparation and incipient-to-wetness impregnation steps of catalyst preparation.

- Catalytic Reaction System: The system consisted of a feed section including mass flow controllers for controlled input of reactant, HPLC pump for water feed and a mixing zone; a reaction section composed of a continuous flow fixed-bed microreactor in a furnace, where the temperature of catalyst bed was controlled by programmable temperature controller.

- Product Analysis System: The quantitative analysis of the reactant and product streams made via gas chromatographs connected on-line to the microreactor flow system.

3.2.1. Catalyst Preparation Systems

Catalyst preparation system seen in Figure 3.1 is used to prepare catalyst via incipient-to-wetness impregnation technique and includes a Retsch UR1 ultrasonic mixer, a vacuum pump, a Buchner flask and a MasterFlex computerized-drive peristaltic pump.

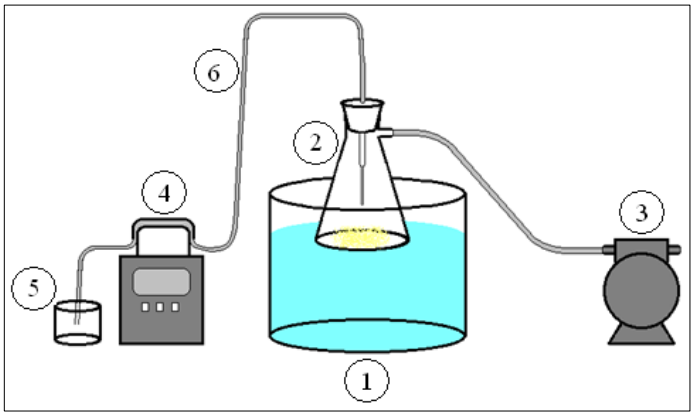

Figure 3.1. Schematic diagram of the impregnation system (Gökaliler, 2012)
(1) Ultrasonic mixer, (2) Buchner flask, (3) Vacuum pump, (4) Peristaltic pump,
(5) Precursor solution, (6) Silicone tubing

Catalysts used in this study were prepared by incipient-to-wetness impregnation method that has three steps:

- Evacuating the support,
- Contacting the support with the precursor solution, and
- Drying.

In this method, certain amount of support was placed in the Buchner erlenmeyer and kept under vacuum both before and during the addition of precursor solution in order to remove trapped air in pores and let the precursor solution to penetrate into pores. First, the support material was mixed with ultrasonic mixer for 30 min. A MasterFlex computerized-drive peristaltic pump was used to add the precursor solution to the vacuum flask at a rate of 0.5 ml/min through silicone tubing. The slurry was mixed during and after impregnation for an extra 90 min for uniform metal dispersion. The thick slurry obtained was dried overnight to remove water.

3.2.2. Catalytic Reaction System

The catalytic reaction system used in this study was designed and constructed in the Catalysis and Reaction Engineering Laboratory of Chemical Engineering Department (CATREL), Boğaziçi University. This system has three main parts: feed, reaction and product analysis.

The OSR reaction system originally designed with two consecutive reactors in order to enable testing the response of WGS catalyst, which is placed in the second reactor, performance to the changes in OSR feed composition as in Figure 3.2. However, for this study, which focuses on the performance and the kinetics of Pt-Ni catalyst in OSR of methane, only the first reactor is used to perform OSR reaction.

The feed section was composed of mass flow control systems, 1/4’’, 1/8’’ and 1/16’’ stainless steel (SS) tubing, valves and fittings to feed gaseous species, i.e. nitrogen, oxygen, methane, and hydrogen and liquid water. Gaseous species were supplied from pressurized cylinders passing through pressure regulators. The flow rates of the gasses were controlled by Brooks Instrument mass flow controllers and the set values were adjusted by two Brooks Instrument 0154 series control boxes. Exit of mass flow controllers was controlled via on-off valves to avoid possible back-pressure fluctuations. Each gas was fed from an independent line according to its defined volumetric flow rate value. Gas mixture could be diverted to the reactor or the bypass line by use of a three way valve. Bypass line also divided into two line; one to send feed mixture for analysis skipping reactor and the other one is the purge line let the feed mixture to come equilibrium.

A Jasco PU-2089 Plus quaternary gradient pump was utilized for water introduction to the system at constant flow rates. Water line had 1/16'' SS tubing and to feed water in gaseous state, whole reactant mixing zone were kept at 135±5 °C using a heating tape, a 16-gauge wire K type sheathed thermocouple and Shimaden SR91 temperature controller. Ceramic wool insulation was covered heated region to reduce heat loss.

Reaction sections were composed of two 47 cm×20 cm×20 cm furnaces with 3.4 cm OD each controlled by a Shimaden FP23 programmable temperature controller, a K-type sheathed thermocouple and a down-flow, 56 cm long 1/4'' OD SS tubular microreactor. The catalyst beds were stabilized by silane treated glass wool in the center of the reactors. Ceramic glass wool insulations were placed in top and bottom ends of the reactors furnace in order to prevent heat loss and provide a stable temperature profile. The reactants prepared with desired feed ratio and mixed enough were allowed to flow to the first reactor. Exit of the first reactor was possible to feed to the second reactor or as already done in this study directed to gas chromatographs to determine product composition. Since product stream contains steam and it is harmful for Molecular Sieve 5A gas chromatograph (GC) column, two cold traps were placed before GC inlet to condense water. The line between reactor exit and cold trap was also heated to prevent steam condensation along the line.

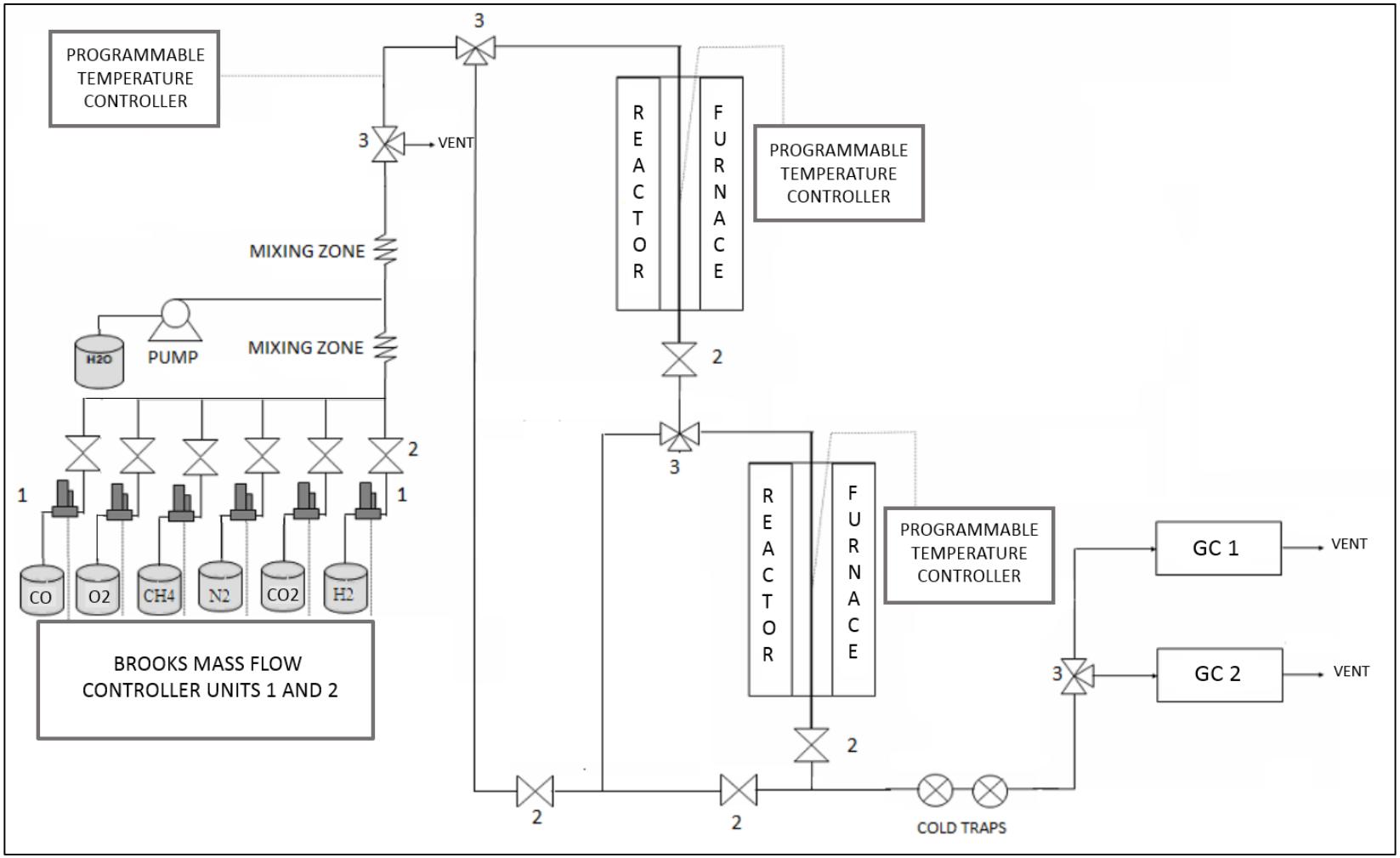

Figure 3.2. Schematic representation of OSR reaction system (Gökaliler, 2012). (1) Mass flow controller, (2) On-off valve, (3) Three-way valve.

3.2.3. Product Analysis System

Two parallel Agilent Technologies 6850 Gas Chromatographs (GCs) equipped with Molecular Sieve 5A and Porapak Q columns were used for analysis of feed and product gas mixtures in reaction system. Analysis conditions of the GCs are given in Table 3.4.

Table 3.4. Gas analysis conditions for OSR analysis system.

	GC 1	**GC 2**
Column packing material	Molecular sieve 5A	Poropak Q
Column temperature	40 °C	40 °C
Column length x ID	2 m x 3 mm	2 m x 3 mm
Carrier gas	Argon	Helium
Carrier gas flow rate	25 ml/min	20 ml/min
Detector type	TCD	TCD
Detector temperature	150 °C	150 °C
Inlet temperature	120 °C	110 °C
Sample loop volume	1 ml	1 ml
Gases analyzed	H_2, N_2, CH_4, O_2, CO	N_2, CH_4, CO_2

The both GCs were calibrated prior to the performance and kinetics experiments. In the preparation of the calibration curve, known volumes of gases were fed and peak areas were measured under the conditions given in Table 3.4. Volume percent versus peak area curves were drawn and estimation factors were determined by linear regression.

3.3. Catalyst Preparation and Pretreatment

In this thesis, two catalysts, 0.2Pt-10Ni/δ-Al_2O_3 and 0.3Pt-10Ni/δ-Al_2O_3, were prepared which gave the highest performance in OSR methane and propane tests conducted by Gökaliler, 2012.

Pellet form γ- Al_2O_3 support material was crushed and sieved to 250-354 μm (45-60 mesh) particle size. After drying γ- Al_2O_3 at 150 °C for 2 h and then calcining it at 900 °C for 4 h in a muffle furnace, thermally stable δ- Al_2O_3 support was obtained.

A sequential impregnation route was applied in the preparation of bimetallic Pt-Ni/δ-Al_2O_3, in which Pt solution was impregnated over initially prepared and calcined Ni/δ-Al_2O_3 catalyst. Ni was impregnated on δ-Al_2O_3 support using an aqueous solution of $Ni(NO_3)_2.6H_2O$ precursor as explained in Section 3.2.1. The precursor solutions were prepared by dissolving the calculated amount of the precursor salt in deionized water with the ratio of ca. 1 ml solution/g support. The resulting slurry was then dried overnight at 120 °C and calcined at 600 °C for 4 h to obtain NiO/δ-Al_2O_3. Similarly, Pt solution prepared using $Pt(NH_3)_4(NO_3)_2$ as a precursor was added to NiO/δ-Al_2O_3 and the resulting slurry was dried overnight at 120°C and calcined at 500 °C for 4 h.

In order to activate catalyst in-situ reduction was conducted before each experiment to reduce oxide states of metals to the metallic state. After placing the certain amount of catalyst into the constant temperature zone of the microreactor, hydrogen with 20 ml/min flow rate was allowed to flow through catalyst bed. Reduction was started by heating the catalyst from room temperature to 150 °C at a rate of 10 °C/min. The catalyst bed was hold at constant temperature of 150 °C for 30 min to remove adsorbed water. Third step was heating the sample from 150 °C to 300 °C at a rate of 5 °C/min, followed by a 30 min isothermal segment at 300 °C for the removal of crystalline water. The temperature was then increased from 300 °C to 500 °C at a rate of 2 °C/min and finally kept constant at 500 °C for 4 h. After reduction, the system was allowed to cool under H_2 flow up to 150 °C and below that temperature N_2 flow was allowed to sweep catalyst surface.

3.4. Reaction Tests

3.4.1. Blank Tests

Blank tests were performed to ensure that the material of construction, glass-wool and δ-alumina (support of the catalysts) have no catalytic activity. The results indicated that these items were inactive under the reaction conditions.

3.4.2. OSR of Methane Performance Tests

All OSR performance experiments were conducted in the first reactor of the system shown in Figure 3.2. After pretreatment period ends, the catalyst bed was brought to reaction temperature under inert flow. The reactants were mixed for 1.5 h and introduced to the catalyst bed according to specified experimental conditions. Two catalysts prepared with different metal loadings, 0.2Pt-10Ni/δ-Al_2O_3 and 0.3Pt-10Ni/δ-Al_2O_3, were used with amount of 150 mg for all performance tests. Experimental conditions of steam-to-carbon ratio (S/C), carbon-to-oxygen ratio (C/O_2) and catalyst weight-to-total flow rate ratio (residence time) given in Table 3.5 and corresponding feed flows in Table 3.6 were applied considering study of Gökaliler, 2012.

Table 3.5. Conditions for OSR of methane performance tests (Gökaliler, 2012).

Set #	**S/C**	**C/O_2**	**W/F (mg cat s ml^{-1})**
1	3	2.12	0.80
2	3	2.12	1.12
3	3	1.50	0.51
4	3	2.70	0.51
5	3	2.12	0.51

Table 3.6. Flow rates of reactants for OSR of methane performance tests (Gökaliler, 2012).

Set #	Reactant Flow Rates (ml/min)			
	Oxygen	**Methane**	**Steam**	**Nitrogen**
1	14.0	29.8	89.6	52.6
2	10.1	21.5	63.8	38.1
3	27.4	40.1	123.5	102.8
4	18.9	51.0	152.1	71.1
5	22.2	47.1	139.8	83.5

In this thesis work, effects of metal loadings in catalyst, C/O_2 ratio and temperature were studied and the performance tests were summarized in Table 3.7.

Table 3.7. Summary of OSR of methane performance tests.

Catalyst	Catalyst weight (mg)	Temperature (°C)	Set #
0.2Pt-10Ni/δ-Al_2O_3	150	450	1
	150	450	2
	150	450	3
	150	450	4
	150	450	5
	150	400	5
	150	350	5
0.3Pt-10Ni/δ-Al_2O_3	150	450	1
	150	450	2
	150	450	3
	150	450	4
	150	450	5
	150	400	5
	150	350	5

3.4.3. OSR of Methane Kinetic Preliminary Tests

After performance tests over two Pt-Ni/δ-Al_2O_3 catalysts were completed, optimal conditions for kinetic experiments were tried to be found for 0.2Pt-10Ni/δ-Al_2O_3 catalyst. The essential criteria of preliminary kinetic study was to minimize methane conversions achieved in order to guarantee that kinetic studies were performed in kinetically controlled region.

The first step was to decrease catalyst weight from 150 mg to 10 mg at 450 °C for Set 5 conditions (Figures 3.5 and 3.6). Since conversion levels were not reduced to desired values, same experiments were repeated at lower temperatures, at 400 and 375 °C. The result of the experiment conducted at 375 °C was satisfactory; therefore, the same experiment was repeated with 20 mg catalyst to confirm linearity of conversion – W/F relation.

Finally, the gas and water volumetric flow rate values were determined considering 10 mg catalyst weight and the targeted S/C and C/O_2 feed ratios for 202.2 ml/min total flow. In this context, C/O_2 ratio was changed from 1.5 to 5.0 and S/C from 2.0 to 4.0 as seen in Table 3.8.

Table 3.8. List of kinetic preliminary experiments with changing feed ratios performed over 0.2Pt-10Ni catalyst.

	C/O_2	**S/C**
Effect of C/O_2	1.5	3.0
	2.0	3.0
	3.0	3.0
	3.5	3.0
	4.0	3.0
	4.5	3.0
	5.0	3.0
Effect of S/C	3.0	2.0
	3.0	2.5
	3.0	3.0
	3.0	4.0

3.4.4. OSR of Methane Kinetic Tests

Kinetic tests were performed to determine the power law type of rate expression of 0.2Pt-10Ni catalyst in the oxidative steam reforming of methane as a function of temperature and partial pressures of methane, oxygen and steam.

Kinetic experiments were performed under differential conditions at atmospheric pressure where reactants - namely methane, oxygen, and steam, were mixed with nitrogen to keep a constant total flow rate of 202 ml/min at 375 °C. The tests for activation energy calculations were conducted also at 350, 400 and 425 °C. In order to ensure that experiments occurred in kinetically controlled region, conversions were tried to be kept low; therefore, small amounts of catalysts (10 or 15 mg) were placed into the reactor.

The feed ratios for kinetic study were designed such that the limits of the S/C changed from 2.03 to 3.08 and C/O_2 from 4.00 to 7.34 to keep the conversion change-residence time relation linear meaning that reactions took place in kinetically controlled region. In the

kinetic experiments, 6 different partial pressure values for each reactant (i.e. methane, oxygen, steam) at two different W/F values (three when the origin is included) were used. The list of the parameters used in the kinetic experiments were given in Table 3.9. Rate orders with respect to methane, oxygen and steam were calculated by application of non-linear regression to the “methane conversion versus residence time” data. For the activation energy calculations, Set 4a was chosen because of its commonly used feed ratio parameters.

Table 3.9. List of kinetic experiments performed over 0.2Pt-10Ni catalyst.

Set #		Catalyst weight (mg)	Partial Pressures (kPa)			
			CH_4	O_2	H_2O	N_2
1	a	10	15.21	3.80	46.28	36.04
	b	15	15.21	3.80	46.28	36.04
2	a	10	16.71	3.80	46.28	34.54
	b	15	16.71	3.80	46.28	34.54
3	a	10	18.36	3.80	46.28	32.89
	b	15	18.36	3.80	46.28	32.89
4	a	10	19.77	3.80	46.28	31.48
	b	15	19.77	3.80	46.28	31.48
5	a	10	21.27	3.80	46.28	29.98
	b	15	21.27	3.80	46.28	29.98
6	a	10	22.80	3.80	46.28	28.45
	b	15	22.80	3.80	46.28	28.45
7	a	10	19.77	2.69	46.28	32.59
	b	15	19.77	2.69	46.28	32.59
8	a	10	19.77	2.99	46.28	32.29
	b	15	19.77	2.99	46.28	32.29
9	a	10	19.77	3.37	46.28	31.91
	b	15	19.77	3.37	46.28	31.91
10	a	10	19.77	4.11	46.28	31.17
	b	15	19.77	4.11	46.28	31.17
11	a	10	19.77	4.49	46.28	30.79
	b	15	19.77	4.49	46.28	30.79
12	a	10	19.77	4.67	46.28	30.61
	b	15	19.77	4.67	46.28	30.61
13	a	10	19.77	4.11	47.64	29.81
	b	15	19.77	4.11	47.64	29.81
14	a	10	19.77	4.11	50.66	26.79
	b	15	19.77	4.11	50.66	26.79
15	a	10	19.77	4.11	53.70	23.75
	b	15	19.77	4.11	53.70	23.75
16	a	10	19.77	4.11	56.74	20.71
	b	15	19.77	4.11	56.74	20.71
17	a	10	19.77	4.11	60.80	16.65
	b	15	19.77	4.11	60.80	16.65

4. RESULTS AND DISCUSSIONS

The aim of the current work is to obtain a reliable power-law type rate expression for oxidative steam reforming of methane over Pt-Ni/δ-Al_2O_3 catalyst valid for practical operating conditions used in a reformer unit of a fuel processor. In this context, first preliminary OSR performance tests were conducted on 0.2Pt-10Ni/δ-Al_2O_3 and 0.3Pt-10Ni/δ-Al_2O_3 systems and the results are comparatively analyzed to see the effect of Pt:Ni ratio on OSR performance. This is followed by preliminary kinetic tests performed on the selected 0.2Pt-10Ni catalyst in order to determine experimental conditions (temperature, S/C and C/O_2 ratios, and W/F) guaranteeing mass transfer limitation free intervals suitable for the kinetic tests. In the final part, kinetic studies were conducted, and the power-law type kinetic expression of OSR over Pt-Ni system was obtained. The experimental work of this thesis is presented in three parts: performance tests over two Pt-Ni, 0.2Pt-10Ni and 0.3Pt-10Ni, catalysts, preliminary kinetic tests, and kinetic tests over the selected catalyst.

4.1. Performance Tests of OSR of Methane over Pt-Ni/δ-Al_2O_3 Catalysts

In the methane OSR performance tests conducted over 0.2Pt-10Ni and 0.3Pt-10Ni catalysts, the experimental parameters used are (i) residence time (W/F), (ii) carbon/oxygen feed ratio (C/O_2), (iii) temperature, and (iv) metal loading, Pt:Ni, ratio.

Experiments listed in Table 3.7 were performed over both catalysts. In all performance tests, catalyst weight was 150 mg, and the residence time values were between 0.51-1.12 mg cat s ml^{-1}. The C/O_2 feed ratio was varied from 1.50 to 2.70 while S/C feed ratio was kept constant as 3.0. During the tests, temperature was kept constant at 450 °C except the tests conducted for studying the effects of temperature; for those, the reaction temperature range used was 350-400 °C. Though time-on-stream (TOS) tests did not indicate any activity loss, 1 h TOS methane conversion data were used for the comparative performance analyses for consistency. The conversion of methane was calculated according to Equation 4.1.

$$Conversion\ \% = \frac{C_{in} - C_{out}}{C_{in}} x100 \quad (4.1)$$

4.1.1. Effect of Residence Time

In order to investigate the effect of residence time on catalyst activity, experimental Sets 1, 2 and 5 in Table 3.5 for W/F values of 0.80, 1.12, and 0.51, respectively, with fixed C/O_2 ratio were conducted over both Pt-Ni catalysts at 450 °C. As can be seen from Figure 4.1, as residence time (W/F) is increased, methane conversion is decreased. The reason might be the active sites of the catalysts can not find enough fresh reactants when the methane flow is lowered at high residence time values.

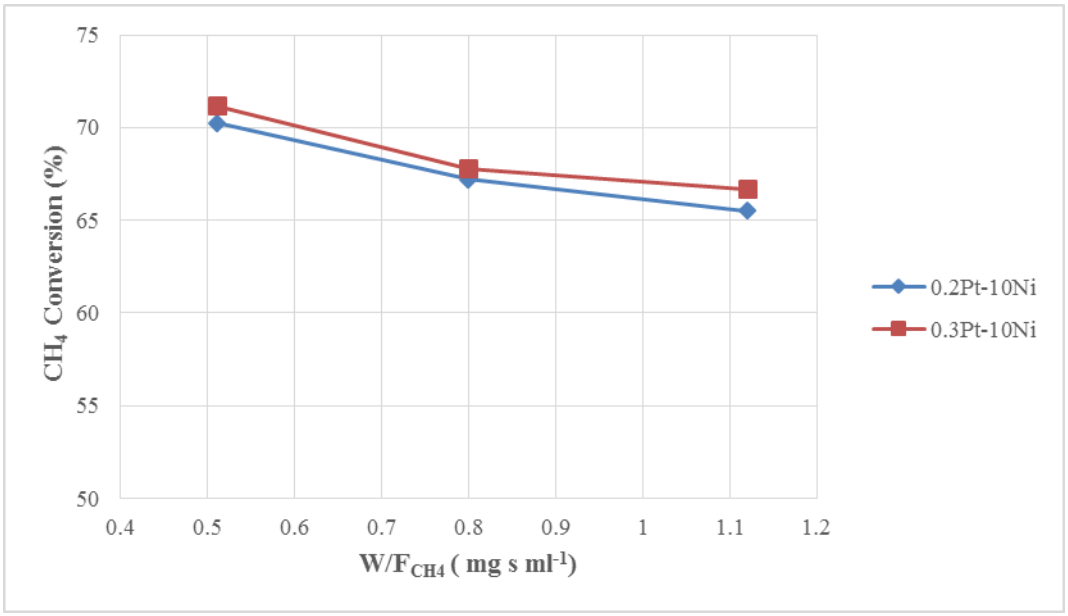

Figure 4.1. Methane conversions over Pt-Ni catalysts at 450 °C for different residence times at constant C/O_2 ratio.

4.1.2. Effect of Carbon/Oxygen Feed Ratio

Effect of oxygen content in feed stream for methane OSR reaction was scrutinized by changing C/O_2 ratio between 1.50 and 2.70 for constant residence time and temperature of 450 °C over two Pt-Ni catalysts via Sets 3, 4, and 5 in Table 3.5.

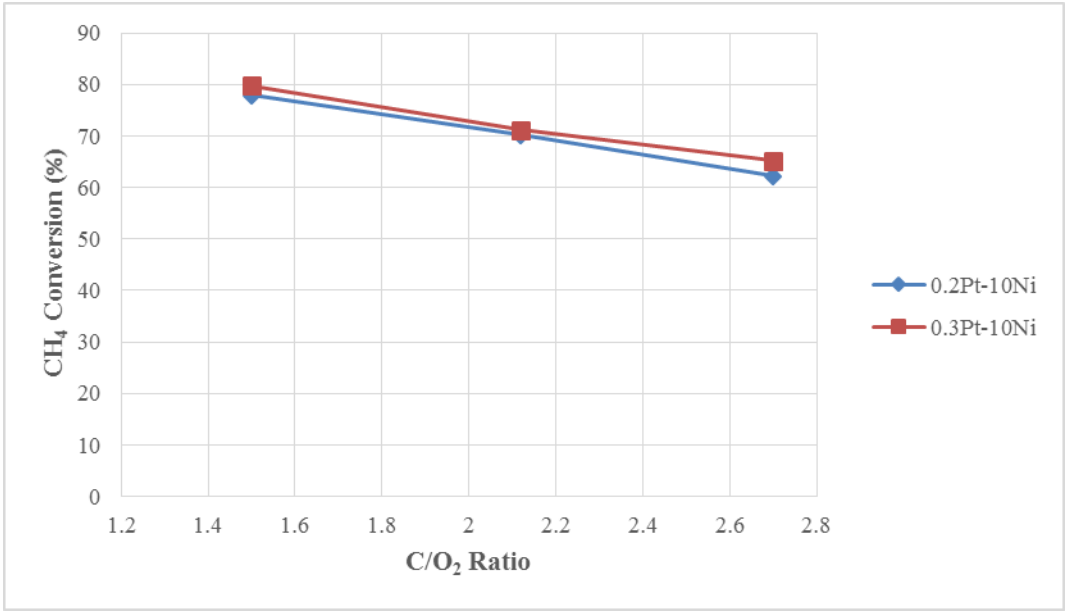

Figure 4.2. Methane conversions over Pt-Ni catalysts at 450 °C for different C/O_2 ratios at constant residence time.

The results showed that feed with lower C/O_2 ratio gives higher conversion for both catalysts as shown in Figure 4.2. This could be explained through two-step mechanism of methane OSR reaction, which are relatively fast exothermic partial/total oxidation followed by endothermic steam reforming (Souza and Schmal, 2005; Ruiz *et al.*, 2008; Escritori *et al.*, 2009). Thus, higher oxygen partial pressure could trigger total oxidation with high exothermicity which favors steam reforming through supplying heat. These two sequential reactions increase methane conversion and also hydrogen production with a similar fashion as well.

4.1.3. Effect of Temperature

As mentioned above, OSR of methane has two step mechanism and the first step, methane oxidation, cannot occur at ambient conditions. Start-up temperature of oxidation, in some references temperature necessary for reaching 10-15% conversion, is called as "light-off temperature", which depends on type of fuel, C/O_2 ratio and type and activity of the catalyst. Because of high thermodynamic stability of methane compared with ethane and propane, it has higher light-off temperature (Shekhawat *et al.*, 2011). Ma *et al.* (1996) have determined light-off temperatures for methane as 316 °C over $Pt/\delta\text{-}Al_2O_3$ catalyst and 364 °C over $Ni/MgO\text{-}Al_2O_3$ catalyst with C/O_2 feeding ratio of 5.0.

Under the light of this information, performance of Pt-Ni samples in methane OSR reaction for Set 5 was tested for temperature range of 350-450 °C as shown in Figure 4.3. As expected, higher methane conversion levels were reached at higher temperatures due to energetics of the OSR process. Increase in temperature was resulted in direct and indirect increase in SR rate, through enhanced TOX yielding higher energy.

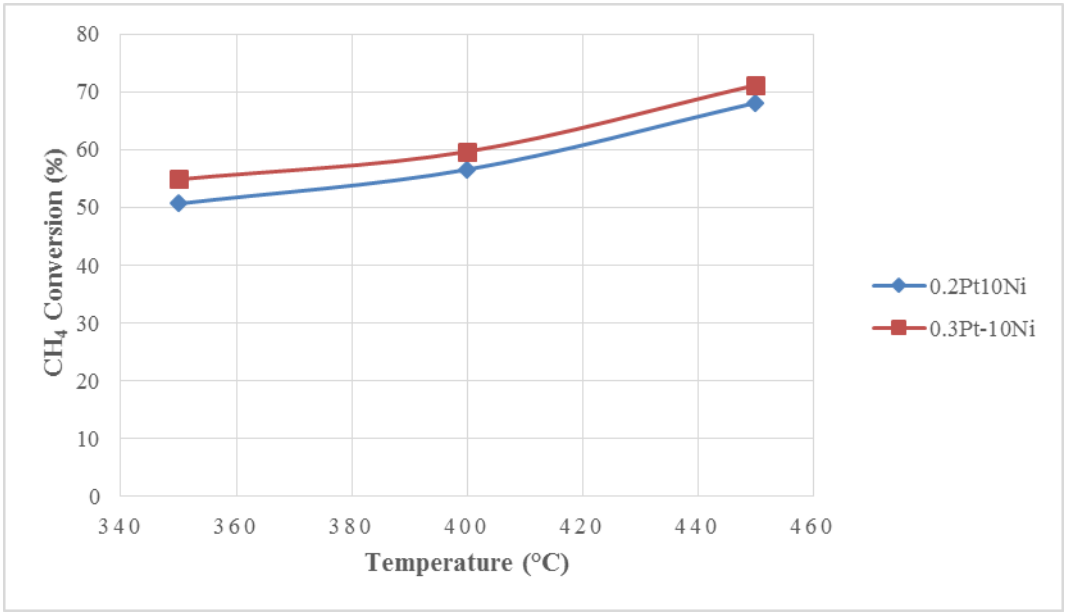

Figure 4.3. Methane conversions over Pt-Ni catalysts for different temperatures at constant C/O_2 ratio and residence time.

4.1.4. Effect of Pt:Ni Metal Loading Ratio

The performance test results obtained through experiments considering W/F, C/O_2 and temperature as the parameters clearly show that the catalyst with higher Pt:Ni ratio gave the higher methane conversion results in all tests (Figures 4.1 - 4.3). However, it could be obviously seen that the difference between the activity levels is not so significant.

In the practical applications of combined FP-FC systems for distributed/dispersed energy production, it is important to use economically feasible and achievable hydrocarbon fuel with well-established distribution network. While propane/butane based LPG seems suitable in the rural areas, methane based natural gas (NG) is more common in the cities owing to its well-established distribution network. Therefore, OSR catalyst should operate with fuel flexibility for methane and propane (Gökaliler, 2012). In the PhD. work conducted by Gökaliler in our group, fuel flexibility of Pt-Ni/δ-Al_2O_3 catalysts were proved for methane-propane feed mixture, and propane OSR kinetic was studied over 0.2Pt-10Ni/δ-Al_2O_3 catalyst. Another reason of selecting 0.2Pt-10Ni for kinetic analysis is the fact that it gives almost the same activity as 0.3Pt-10Ni with less Pt loading. Hence, it was decided to continue OSR kinetic study over the same catalyst, 0.2Pt-10Ni/δ-Al_2O_3.

4.2. Kinetic Preliminary Tests of OSR of Methane over 0.2Pt-10Ni/δ-Al_2O_3 Catalyst

The purpose of the experiments performed in this part is to find the limits of the experimental parameters guaranteeing low conversion levels which ensure the methane OSR kinetic experiments over 0.2Pt-10Ni catalyst would be conducted in kinetically controlled, mass transfer limitation free, region. Therefore, methane conversions were tried to be decreased as much as possible within reasonable reaction conditions.

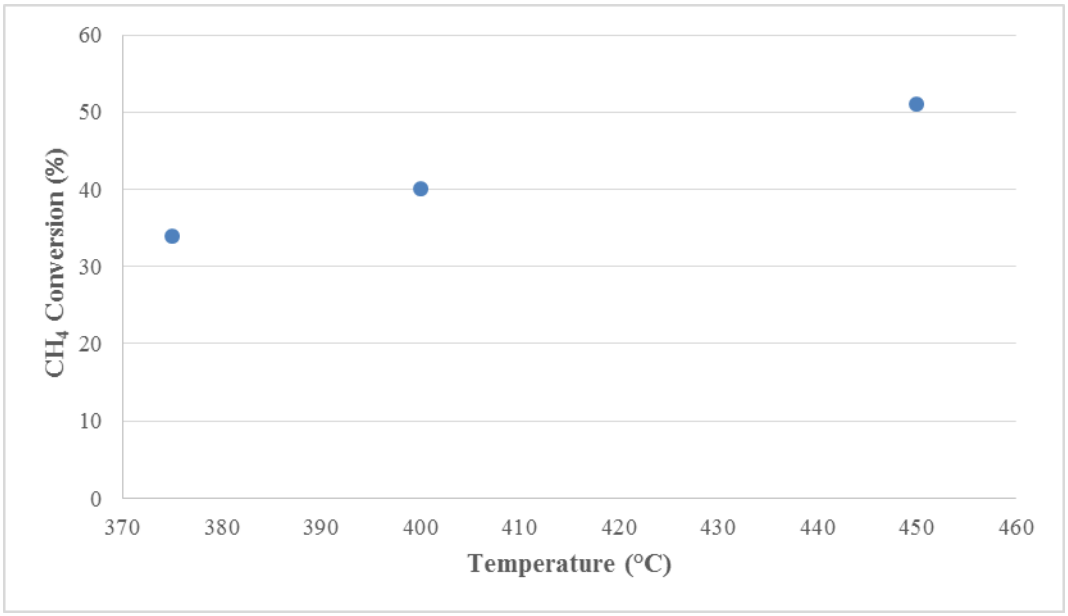

Figure 4.4. Methane conversions over 10 mg 0.2Pt-10Ni catalyst for different temperatures at constant C/O_2 ratio and residence time.

The first change was to reduce catalyst amount from 150 mg to 10 mg at 450 °C for Set 5 conditions, i.e. C/O_2=2.12 and S/C=3.00 (Tables 3.5 and 3.6). As the reaction temperature was decreased from 450 °C to 400 °C and 375 °C, methane conversion was decreased from 51% to 40% and 34%, respectively (Figure 4.4). Kinetic experiments were decided to be continued at 375 °C which is also a practical OSR reactor temperature in FP operation.

It should be noted that kinetic experiments should show linearity in conversion (or reaction rate) versus residence time (or catalyst weight for constant flow rate) graphs. In order to confirm this rule, the experiment conducted at Set 5 conditions and 375 °C over 10 mg catalyst was repeated for 20 mg catalyst weight. It gave acceptable R^2 value of 0.93 (Figure 4.5) and the goodness of fit was found suitable.

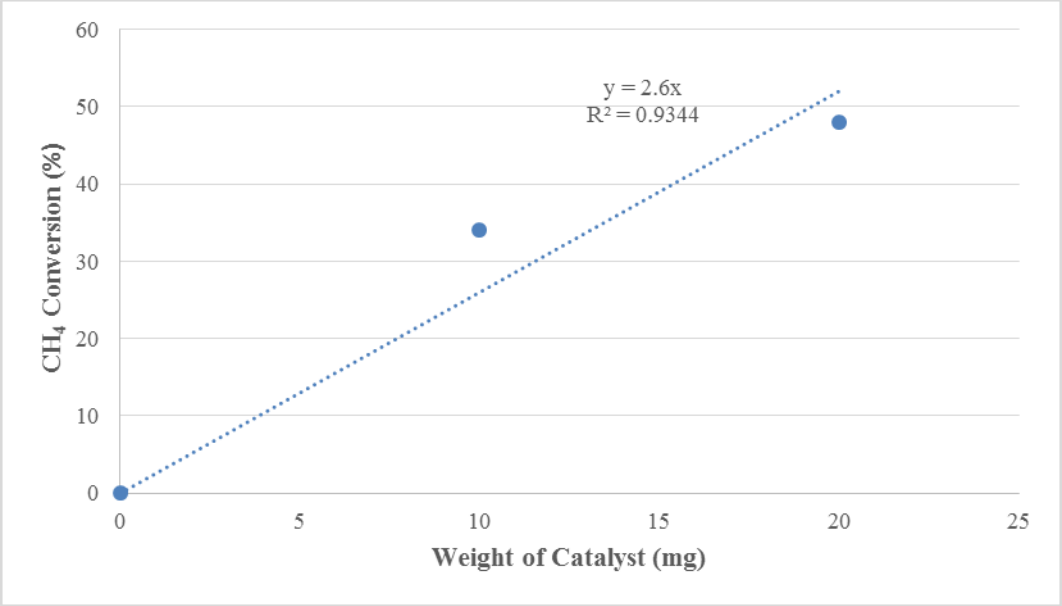

Figure 4.5. Methane conversions over 10 and 20 mg 0.2Pt-10Ni catalyst at constant C/O_2 ratio, residence time, and temperature.

The literature survey conducted within the scope of this thesis pointed out that performance results of methane OSR is strongly affected by feed composition. Thus, in order to decide the ranges for C/O_2 and S/C feed ratios suitable for performing the kinetic tests, methane conversion values were found for parametrically changed feed ratios, according to Table 3.8, at 375 °C by using 10 mg catalyst under 202.2 ml/min total flow rate. In this context, first C/O_2 ratio was changed in a wide range, between 1.5 and 5.0, at constant S/C ratio of 3.0, then S/C ratio was varied from 2.0 to 4.0 at constant C/O_2 ratio of 3.0.

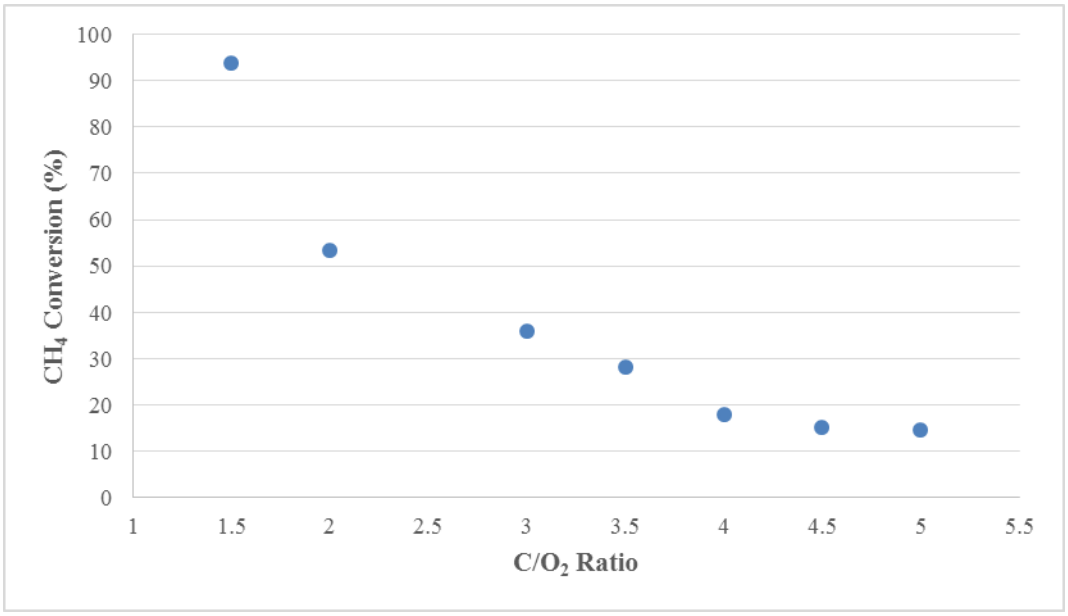

Figure 4.6. Methane conversions over 10 mg 0.2Pt-10Ni catalyst at constant residence time, temperature and S/C feed ratio with changing C/O_2 feed ratio.

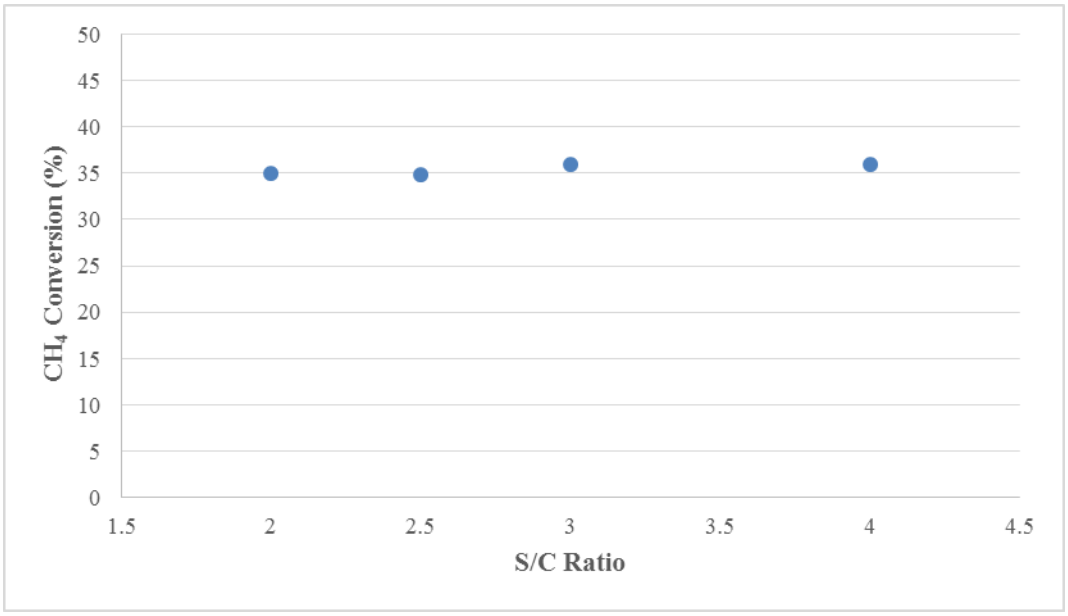

Figure 4.7. Methane conversions over 10 mg 0.2Pt-10Ni catalyst at constant residence time, temperature and C/O_2 feed ratio with changing S/C feed ratio.

Results obtained from this preliminary work on the effects of C/O_2 and S/C feed ratios were presented in Figures 4.6 and 4.7, respectively. According to the results obtained, higher C/O_2 ratio leads to a lower the methane conversion to a large extent, whereas change in S/C ratio does not have a significant effect on methane conversion levels for the parameter ranges tested. As a result, kinetic experiments were decided to be performed for C/O_2 and S/C ratios between, 4.00 and 7.34 and from 2.03 to 3.08, respectively.

4.3. Kinetic Study of OSR of Methane over 0.2Pt-10Ni/δ-Al_2O_3 Catalyst

Kinetic experiments tabulated in Table 3.9 were conducted under 202 ml/min total flow rate at atmospheric pressure and 375 °C unless specified otherwise. The catalyst weight was chosen as 10 and 15 mg to obtain lower conversion values ensuring that the reaction is controlled merely by kinetics.

The initial reaction rates ($-r_{CH4}$) were calculated from methane conversion (x_{CH4}) versus residence time (W/F_{CH4}) data as follows,

$$-r_{CH4} = \frac{dx_{CH4}}{d(W/F_{CH4})} \tag{4.1}$$

where x_{CH4} is methane conversion, F_{CH4} is methane flow rate in μmol s^{-1}, W is catalyst weight in mg, and $-r_{CH4}$ is the reaction rate in μmol mg^{-1} s^{-1}.

Methane consumption rates were obtained from intrinsic kinetic data in the initial rate region by using differential method of analysis, which is one of the most established methods to determine reaction orders and specific reaction rates. The raw experimental data obtained as methane conversion versus residence time plots were given in Appendix A. Initial rates were calculated from the slopes of those plots by differentiating the data and extrapolating it to zero time.

Power-law type of rate expression was applied as in Equation 4.2 as suggested by Berry *et al*. (2006) and Gökaliler *et al*. (2012).

$$-r_{methane} = kP_{methane}^{\alpha}P_{oxygen}^{\beta}P_{steam}^{\gamma} \tag{4.2}$$

$$\ln(-r_{methane}) = \ln(k) + \alpha\ln(P_{methane}) + \beta\ln\left(P_{oxygen}\right) + \gamma\ln(P_{steam}) \tag{4.3}$$

$$k = k_0 e^{\frac{-E_A}{RT}} \tag{4.4}$$

$$\ln(k) = \ln(k_0) - \frac{-E_A}{RT} \tag{4.5}$$

For the evaluation of the parameters, i.e. orders of reaction with respect methane, oxygen and steam – α, β and, γ, respectively – and the rate constant *k*, natural logarithm of Equation 4.2 was taken, and Equation 4.3 was obtained. The initial methane consumption rates were listed in Table 4.1 with corresponding partial pressures of reactants – methane, oxygen and steam – and R^2 values for linear fits.

Table 4.1. Initial rates of methane OSR over the 0.2Pt-10Ni catalyst at 375 °C under conditions defined in Table 3.9.

Set #	P_{CH4} (kPa)	P_{O2} (kPa)	P_{H2O} (kPa)	CH_4 Consumption Rate (µmol mg^{-1} s^{-1})	R^2
1	15.21	3.80	46.28	34.25	0.98
2	16.71	3.80	46.28	45.81	0.93
3	18.36	3.80	46.28	49.17	0.93
4	19.77	3.80	46.28	43.56	0.96
5	21.27	3.80	46.28	44.06	1.00
6	22.8	3.80	46.28	57.29	0.95
7	19.77	2.69	46.28	23.72	0.99
8	19.77	2.99	46.28	37.86	0.98
9	19.77	3.37	46.28	36.36	1.00
10	19.77	4.11	46.28	55.32	0.94
11	19.77	4.49	46.28	64.70	0.93
12	19.77	4.67	46.28	61.28	1.00
13	19.77	4.11	47.64	48.08	0.99
14	19.77	4.11	50.66	55.76	0.92
15	19.77	4.11	53.70	49.78	0.93
16	19.77	4.11	56.74	61.13	0.96
17	19.77	4.11	60.80	61.15	0.99

The rate values obtained from the 17 pairs of experiments (in Tables 3.9 and 4.1) were used to calculate reaction orders with respect to reactants. Reaction orders in Equation 4.2 were estimated by non-linear regression analysis in the MATLAB™ environment and are given in Table 4.2. Reaction rate showed positive dependency for all reactants with a decreasing order of oxygen, methane, and steam as expected.

Table 4.2. Estimated reaction orders for methane OSR over 0.2Pt-10Ni catalyst.

	α	**β**	**γ**
Reaction Orders	0.81	1.60	0.44

As mentioned previously, power-law type of rate expressions for OSR are scarce; therefore, a direct comparison of reaction orders with literature is not possible. Nevertheless, both Berry *et al*. (2006) and Gökaliler *et al*. (2012) found positive dependency for fuel and oxygen partial pressures for OSR kinetics. However, unlike this study, they ended up with a negative dependency for steam partial pressure.

In order to estimate the apparent activation energy (E_A) and the pre-exponential factor (k_0), Arrhenius equation (Equation 4.4) was utilized. Set 4a in Table 3.9, which was conducted at 375 °C, was repeated at 350, 400 and 425 °C, and the results of those experiments were used in the linearized version of Arrhenius equation (Equation 4.5). Plotted data and estimated kinetic parameters based on the results obtained in 350-425 °C temperature range were represented in Figure 4.8 and Table 4.3, respectively.

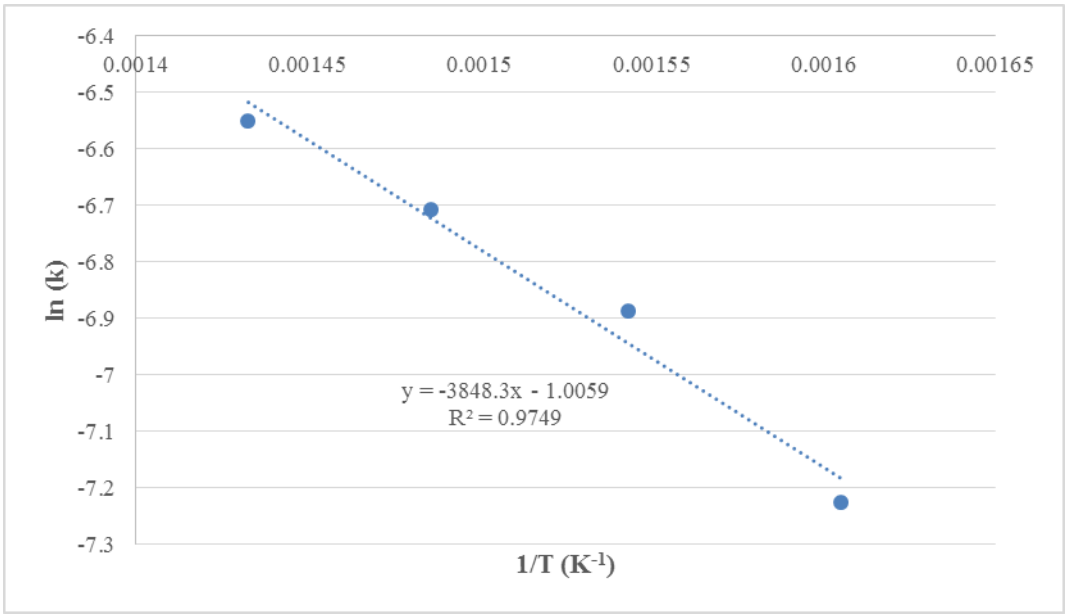

Figure 4.8. Arrhenius plot for methane OSR over 0.2Pt-10Ni/δ-Al_2O_3 catalyst for a temperature range 350-425 °C.

Table 4.3. Kinetic parameters of methane OSR.

Parameter	Units	Estimates
k_0	µmol mgcat^{-1} s^{-1} kPa$^{-2.85}$	0.366
E_A	kJ mol^{-1}	31.99

It should be noted that when the same analysis is performed for a narrower temperature range, 350-400 °C, in order to eliminate any possible effect of reaction path change on k_0 and E_A by keeping the interval within ±25 °C of the temperature of the kinetic tests, the goodness of fit becomes R^2=0.9773 in the ln (k) versus 1/T graph (Figure 4.9) yielding k_0 and E_A values as 0.956 µmol mgcat^{-1} s^{-1} kPa$^{-2.85}$ and 39.05 kJ mol^{-1}, respectively. A comparative analysis between the calculated k_0 and E_A values for these two temperature ranges confirm the high sensitivity of OSR pathway to temperature.

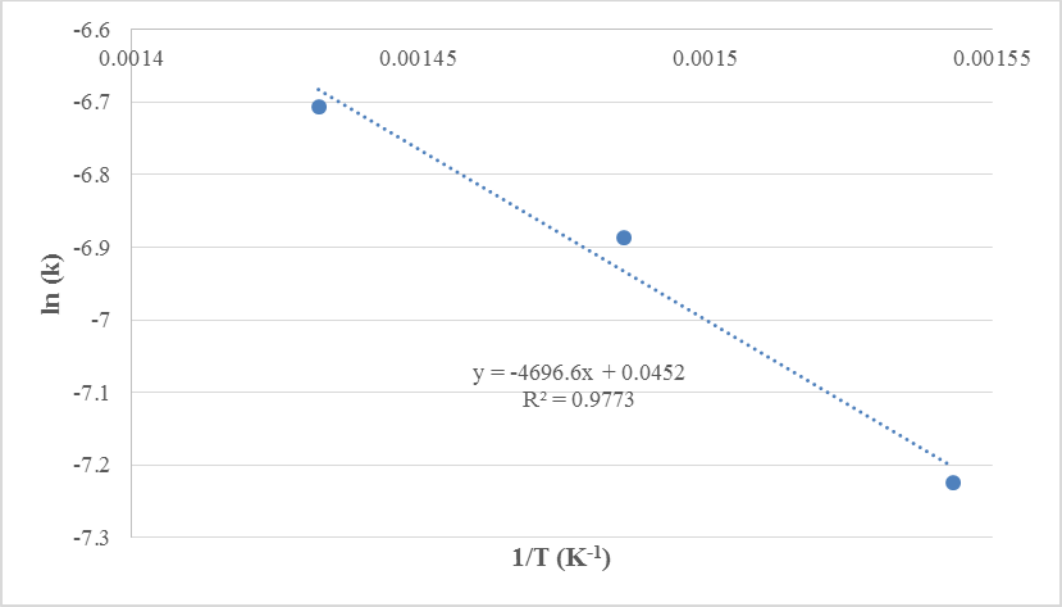

Figure 4.9. Arrhenius plot for methane OSR over 0.2Pt-10Ni/δ-Al_2O_3 catalyst for a temperature range 350-400 °C.

Finally, analysis of rate data was validated by comparing methane conversion rates predicted by the model in Equation 4.2 with the experimental rate values reported in Table 4.1. The corresponding plot in Figure 4.10 shows that derived power-law type rate expression predicts overall methane conversion rates reliably considering high R^2 value, which is an indicator of goodness of fit.

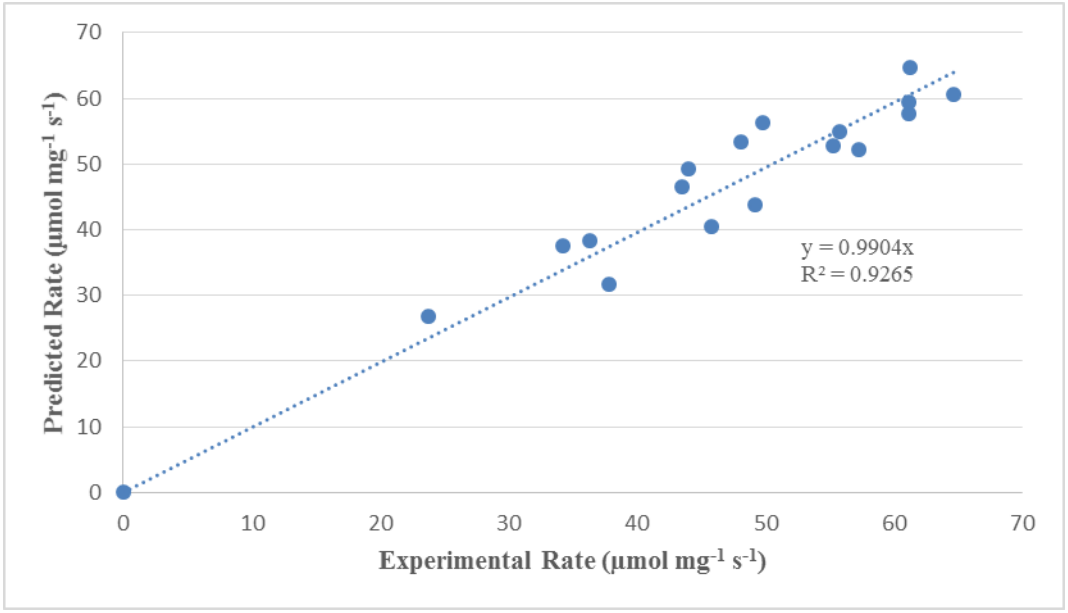

Figure 4.10. Experimental rates versus predicted rates by kinetic model for methane OSR over 0.2Pt-10Ni catalyst.

5. CONCLUSIONS AND RECOMMENDATIONS

5.1. Conclusions

In the current work, the aim was to obtain a reliable power-law type rate expression for oxidative steam reforming of methane over Pt-Ni/δ-Al_2O_3 catalyst valid for practical operating conditions used in a reformer unit of a fuel processor. In this context, preliminary methane OSR performance tests over 0.2Pt-10Ni/δ-Al_2O_3 and 0.3Pt-10Ni/δ-Al_2O_3 systems were conducted first to scrutinize the effects of Pt:Ni ratio and reaction conditions on OSR performance.

Performance tests were conducted by varying residence time, C/O_2 feed ratio, and reaction temperature at constant S/C ratio of 3.0 over 150 mg sample for both catalysts. Residence time values were varied between 0.51-1.12 mg cat s ml^{-1}, and increase in residence time decreased methane conversion most probably due to inadequate fresh reactants on active sites at high residence time values. C/O_2 feed ratio was changed from 1.50 to 2.70 and increase in oxygen content in feed stream triggered exothermic TOX, which favors endothermic SR through energy transfer resulted in higher methane conversion. Temperature was kept constant at 450 °C for the performance experiments except the ones for studying the temperature effects; in those, temperature range was 350-400 °C. Elevated temperatures led higher methane conversion as expected due to energetics of the OSR process. 0.3Pt-10Ni catalyst showed slightly higher methane conversions than 0.2Pt-10Ni for all investigated parameters. However, as fuel flexibility of Pt-Ni/δ-Al_2O_3 catalysts in OSR were proved for methane-propane feed mixture and propane OSR kinetic over 0.2Pt-10Ni system was already studied, it was decided to continue OSR kinetic study over 0.2Pt-10Ni system.

In the preliminary kinetic tests, methane conversions were tried been lowered to ensure mass transfer limitation free intervals suitable for the kinetic tests. Based on the results, kinetic experiments were decided to be continued at 375 °C. Finally, C/O_2 and S/C feed ratios were tested; methane conversion showed highly negative dependency to C/O_2 ratio and almost no dependency to S/C ratio in feed stream.

Kinetic study was performed for determining intrinsic reaction rates of methane OSR over 0.2Pt-10Ni catalyst at 375 °C. Multivariable non-linear optimization function of MATLAB™ was utilized to estimate reaction orders. The proposed power-law type rate expression that is reliable in the range of $2.03 < S/C < 3.08$ and $4.0 < C/O_2 < 7.34$ feed ratios has reaction orders as 0.81, 1.60 and 0.44 in methane, oxygen and steam partial pressures, respectively. The apparent activation energy for methane OSR was calculated as 31.99 kJ mol^{-1} and pre-exponential factor as 0.366 μmol $mgcat^{-1}$ s^{-1} $kPa^{-2.85}$ in the 350-425 °C interval. When the temperature range was narrowed to 350-400 °C, the apparent activation energy and the pre-exponential factor were estimated as 39.05 kJ mol^{-1} and 0.956 μmol $mgcat^{-1}$ s^{-1} $kPa^{-2.85}$, respectively, confirming the high sensitivity of OSR pathway to temperature.

5.2. Recommendations

Regarding the results of present work, following studies are recommended for obtaining further useful results:

- Infrared adsorption experiments for the reactants of OSR reaction in FTIR-DRIFTS system should be performed over 0.2Pt-10Ni/δ-Al_2O_3 catalyst to scrutinize the surface reactions, which is essential for the determination of the plausible reaction mechanism.

- In kinetic study, effects of product gases – H_2, CO_2, and CO – on reaction rate were neglected. Kinetic tests should be performed also for mixed feed conditions.

- Experiments can be performed with more than two residence times in order to obtain higher accuracy.

APPENDIX A: CONVERSION VERSUS RESIDENCE TIME GRAPHS FOR KINETIC TESTS

Methane conversion versus residence time graphs for OSR of methane kinetic study over 0.2Pt-10Ni/δ-Al_2O_3 catalyst are given below for experiments given in Table 3.9.

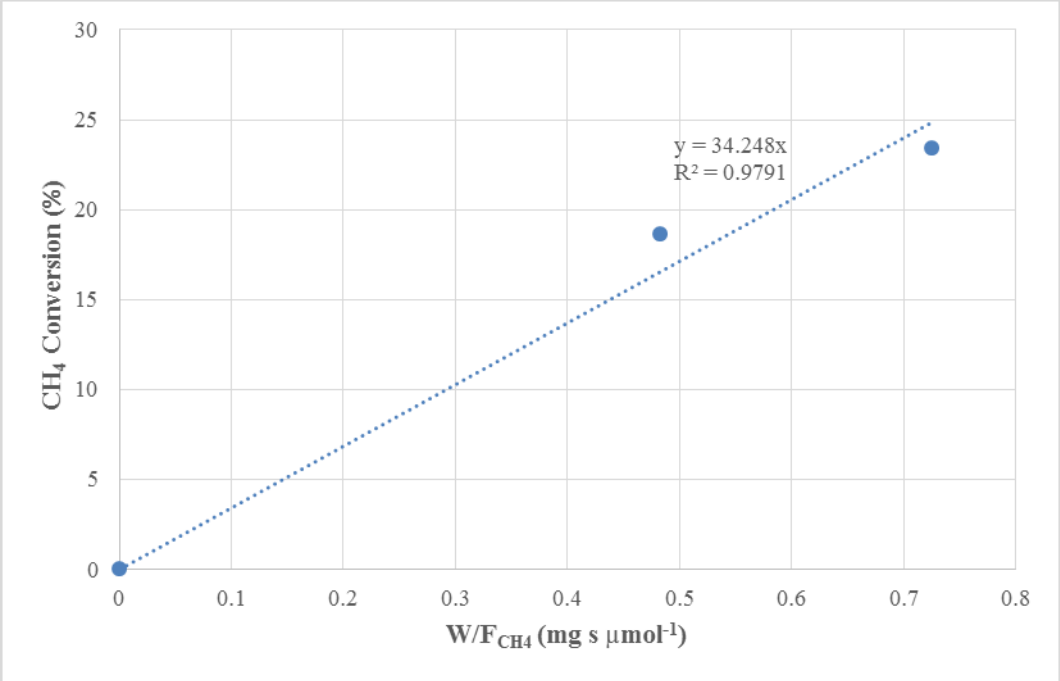

Figure A.1. Percent CH_4 conversion vs. residence time graph for Experiment 1.

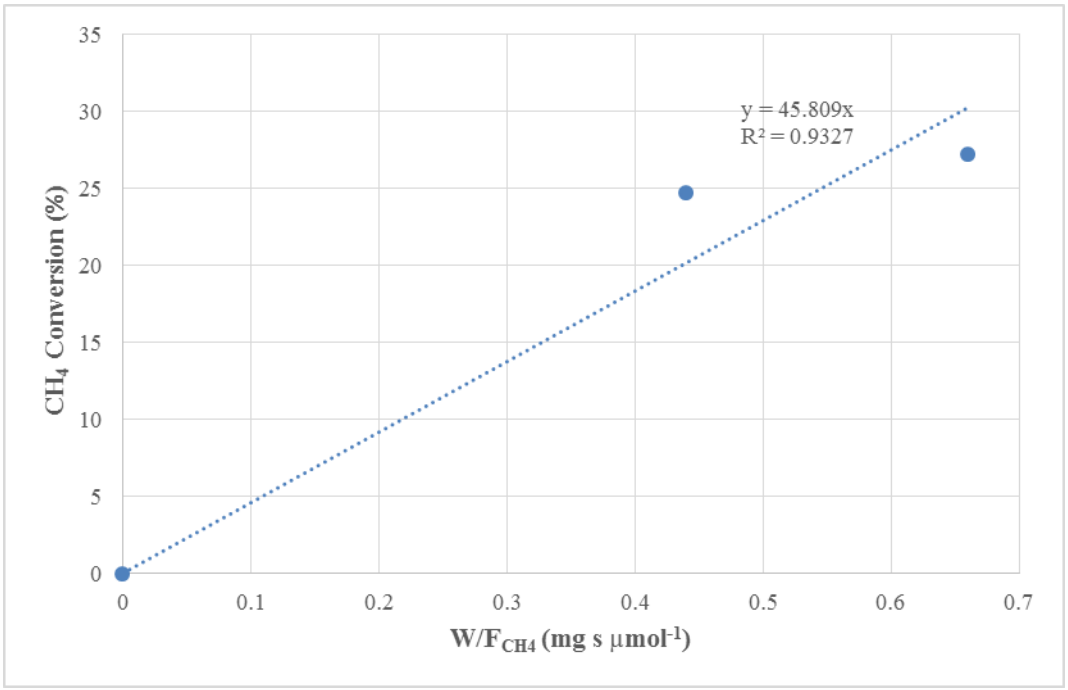

Figure A.2. Percent CH_4 conversion vs. residence time graph for Experiment 2.

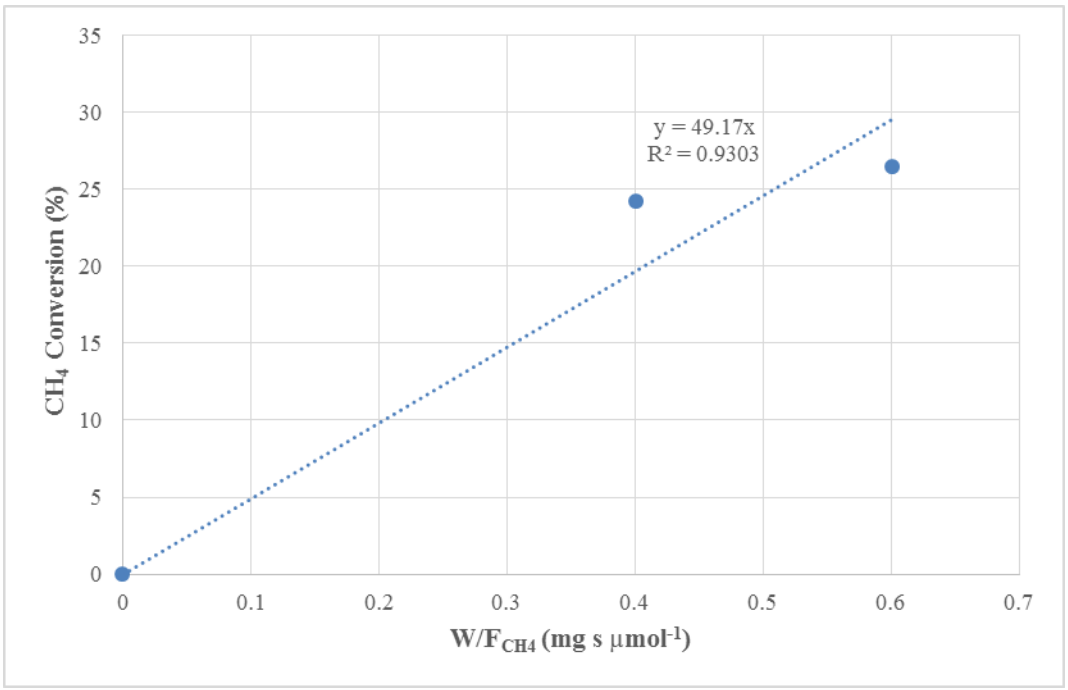

Figure A.3. Percent CH_4 conversion vs. residence time graph for Experiment 3.

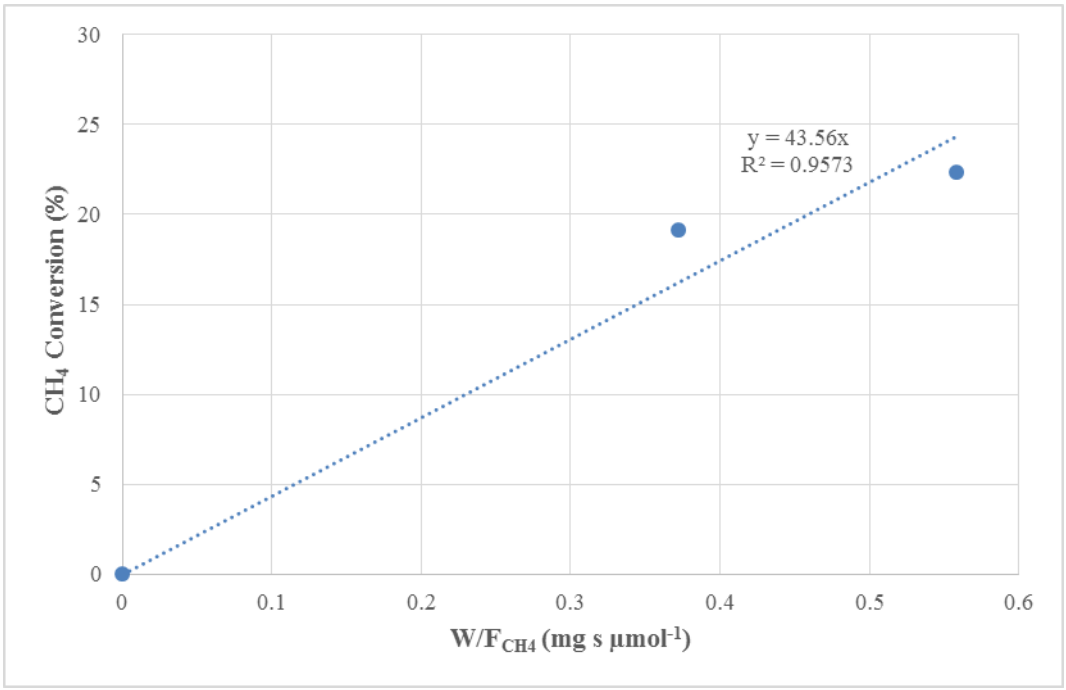

Figure A.4. Percent CH_4 conversion vs. residence time graph for Experiment 4.

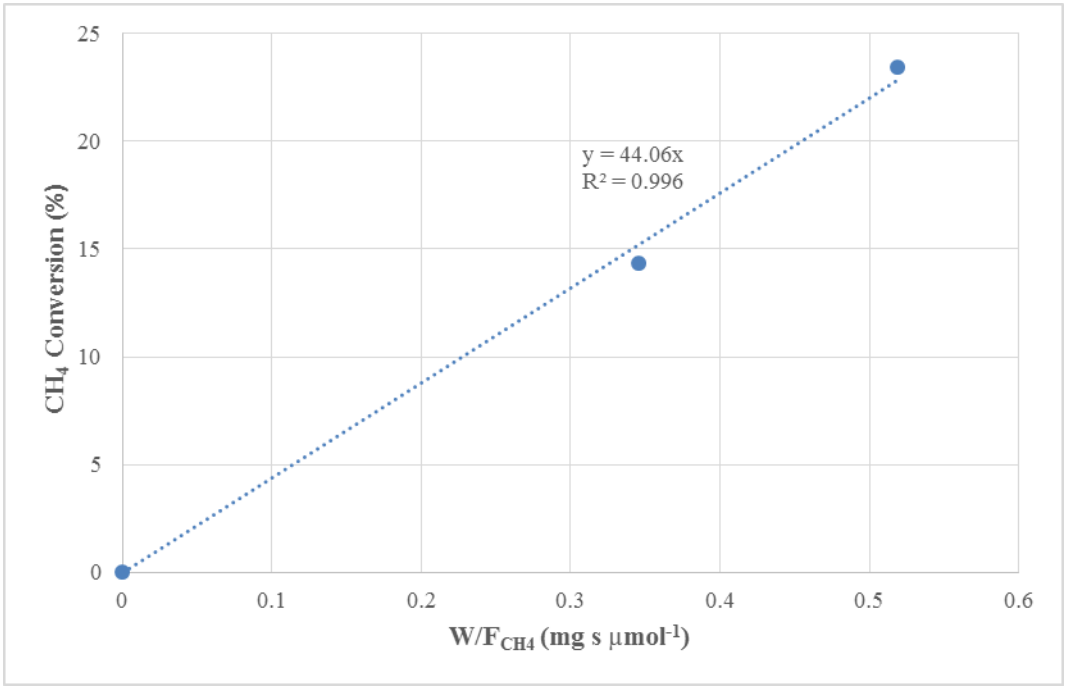

Figure A.5. Percent CH_4 conversion vs. residence time graph for Experiment 5.

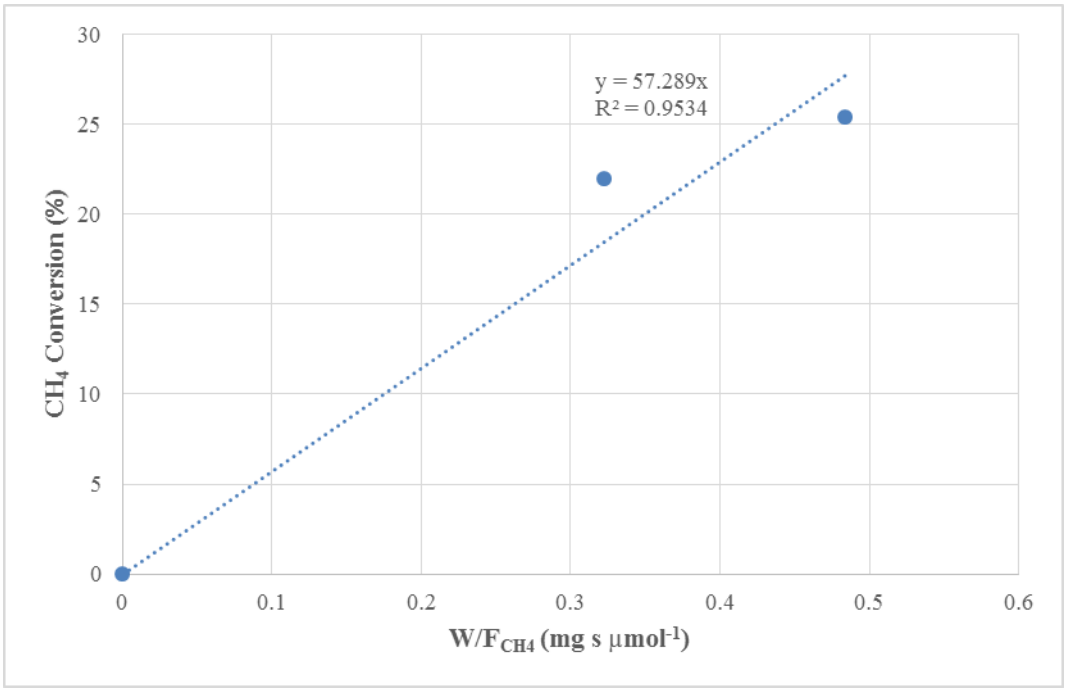

Figure A.6. Percent CH_4 conversion vs. residence time graph for Experiment 6.

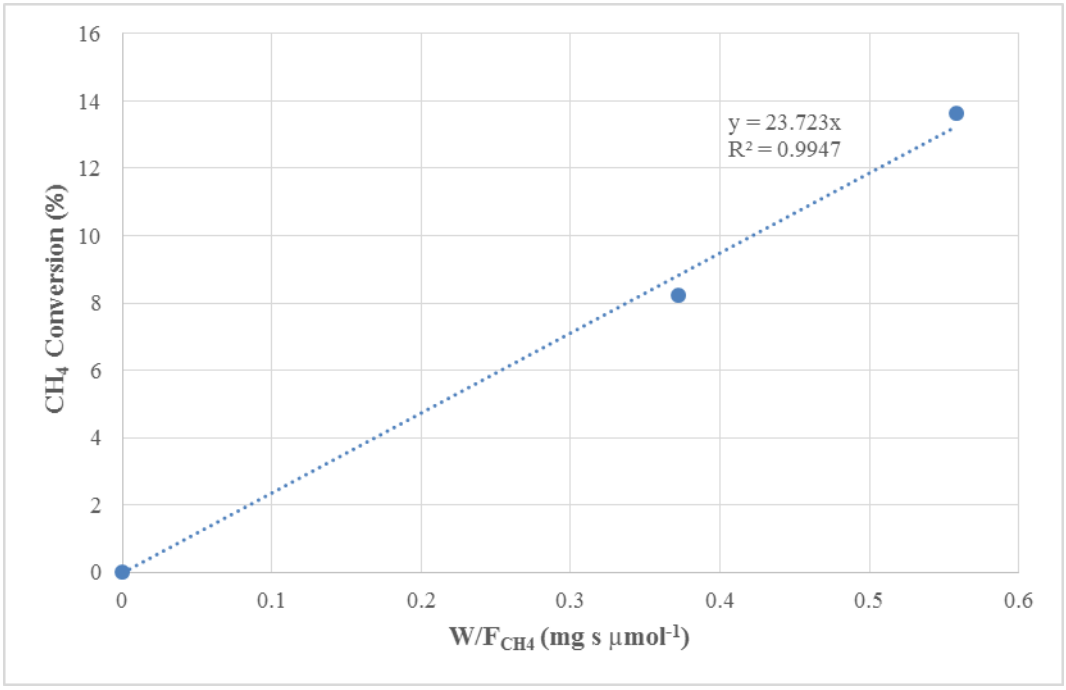

Figure A.7. Percent CH_4 conversion vs. residence time graph for Experiment 7.

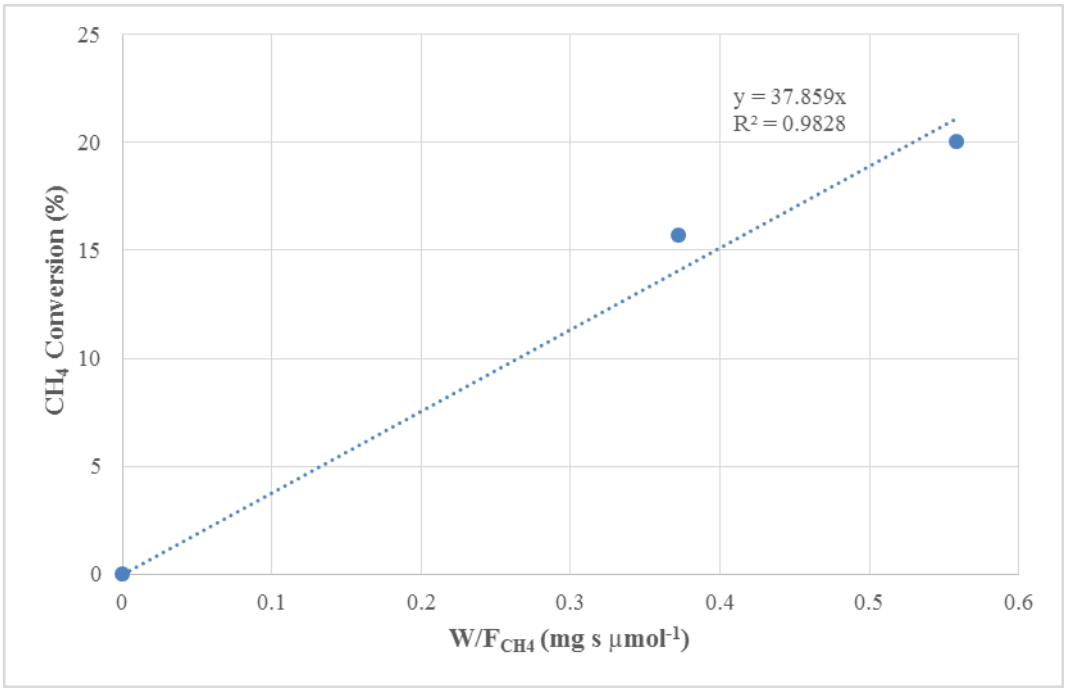

Figure A.8. Percent CH_4 conversion vs. residence time graph for Experiment 8.

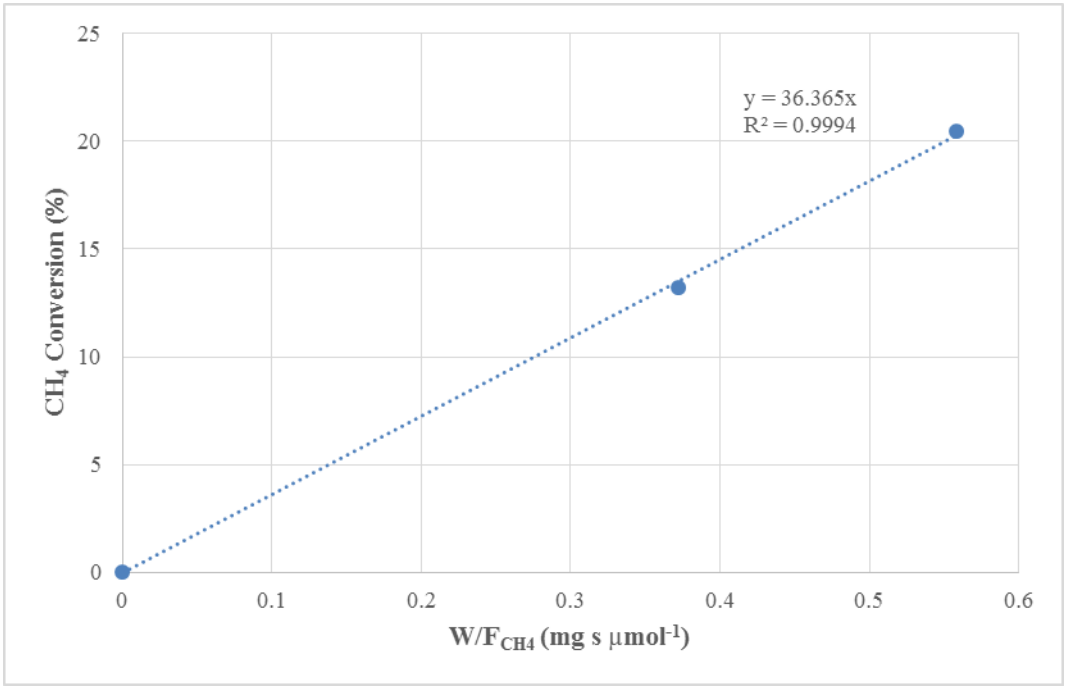

Figure A.9. Percent CH_4 conversion vs. residence time graph for Experiment 9.

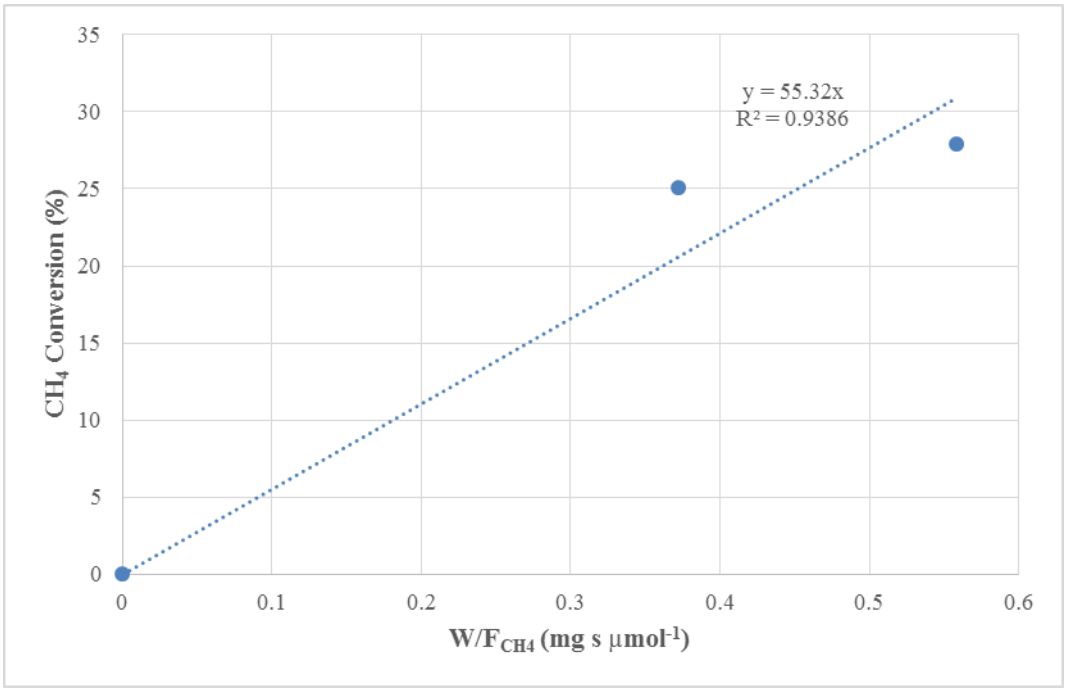

Figure A.10. Percent CH_4 conversion vs. residence time graph for Experiment 10.

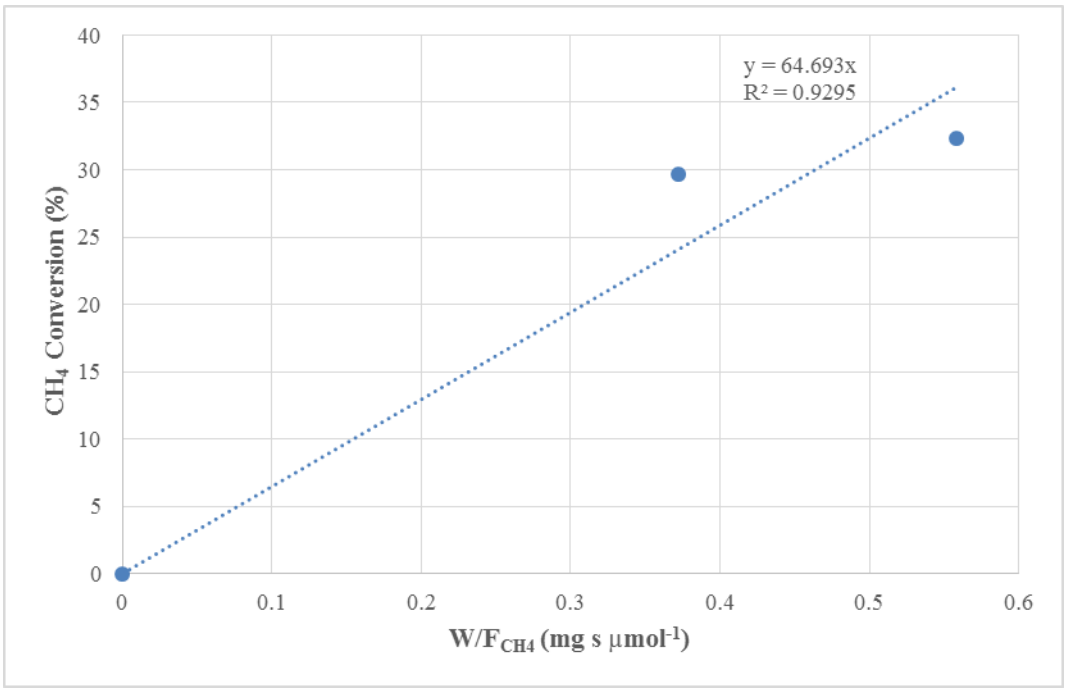

Figure A.11. Percent CH_4 conversion vs. residence time graph for Experiment 11.

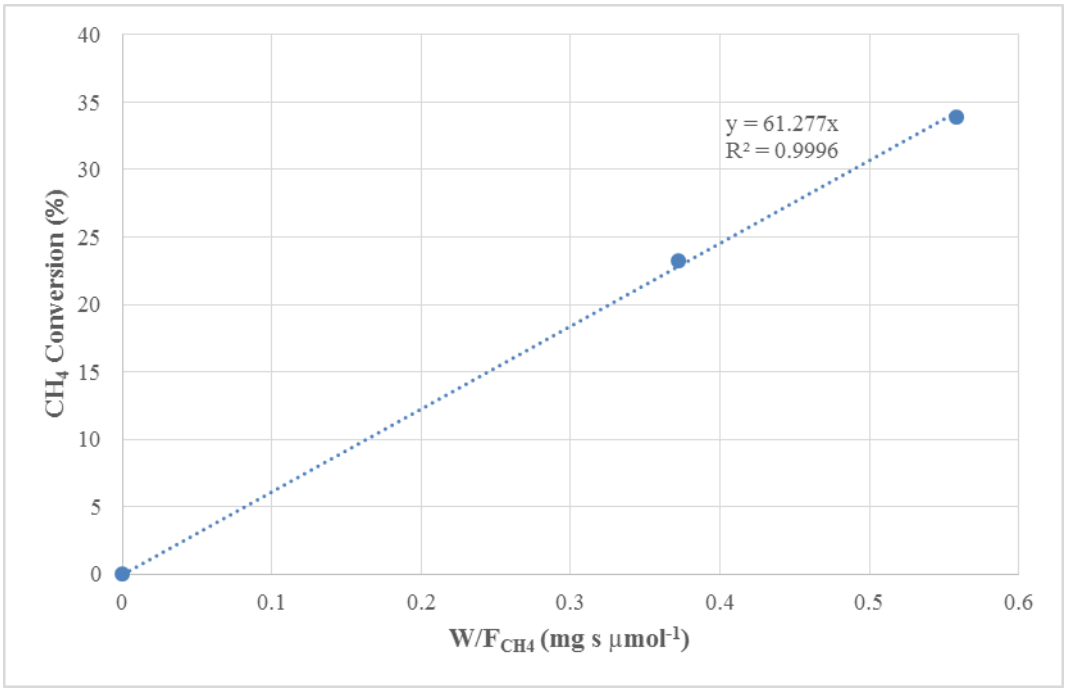

Figure A.12. Percent CH_4 conversion vs. residence time graph for Experiment 12.

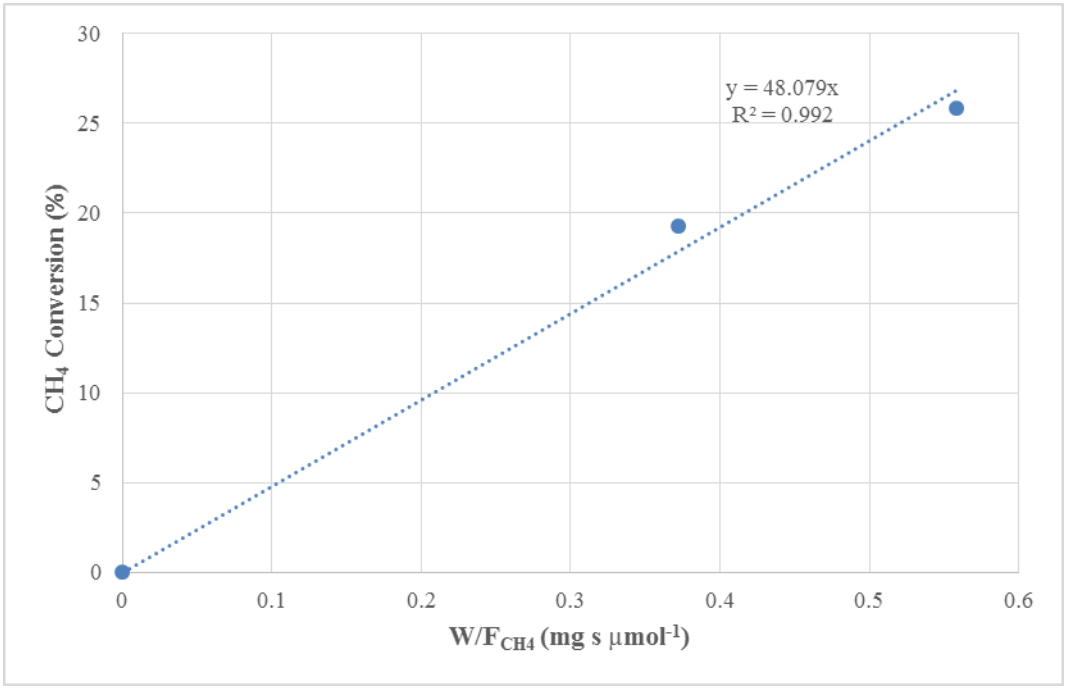

Figure A.13. Percent CH_4 conversion vs. residence time graph for Experiment 13.

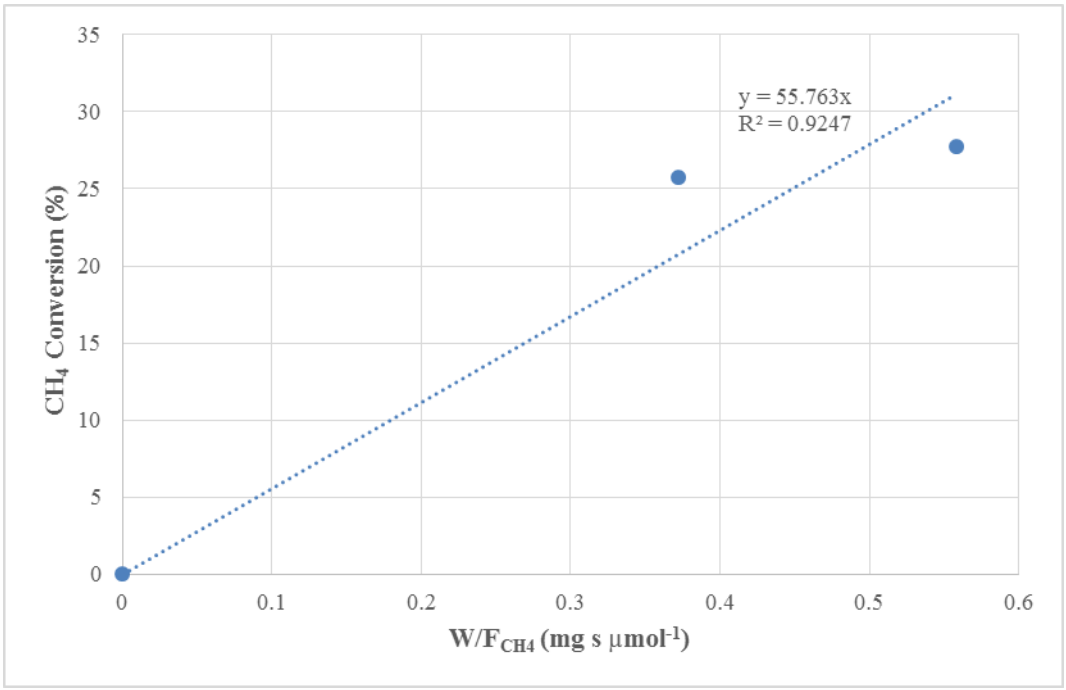

Figure A.14. Percent CH_4 conversion vs. residence time graph for Experiment 14.

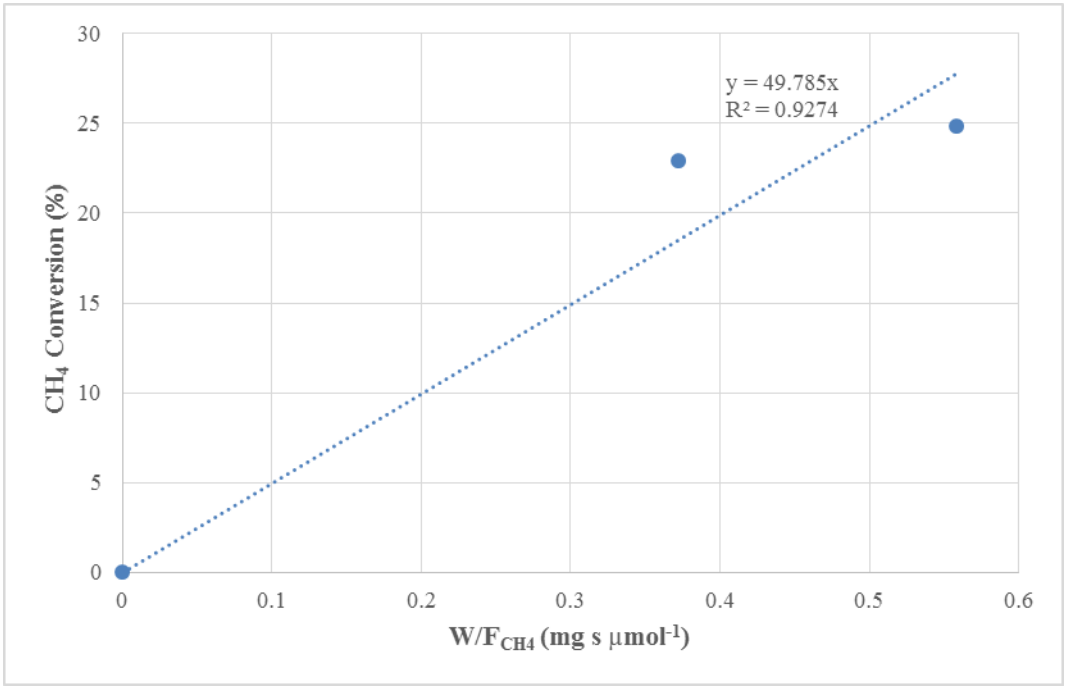

Figure A.15. Percent CH_4 conversion vs. residence time graph for Experiment 15.

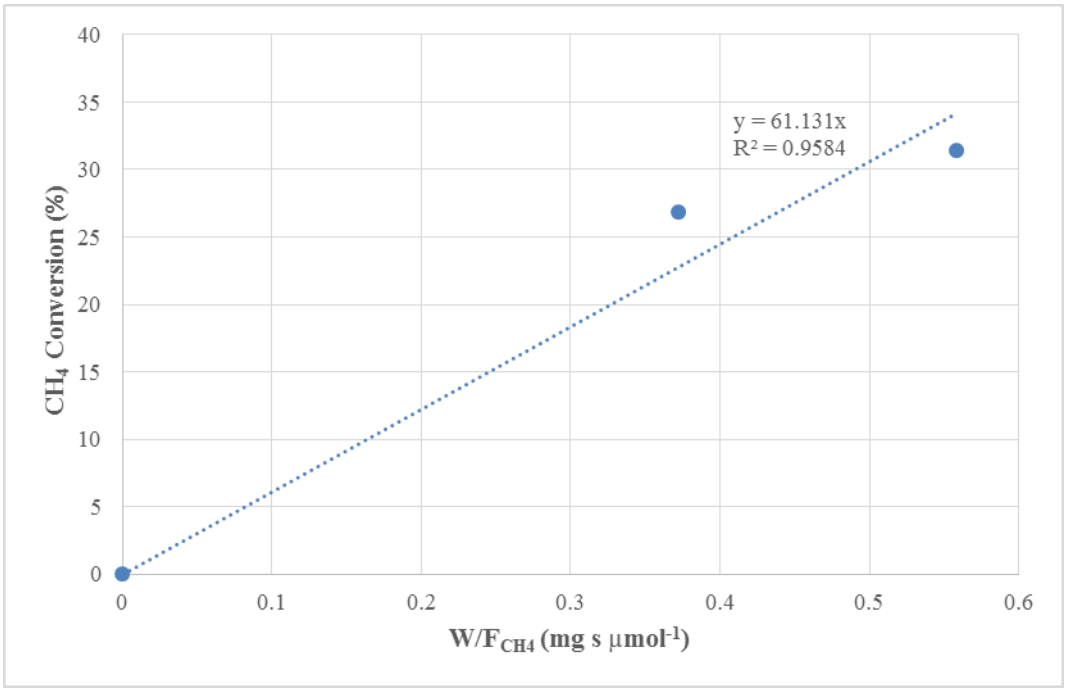

Figure A.16. Percent CH_4 conversion vs. residence time graph for Experiment 16.

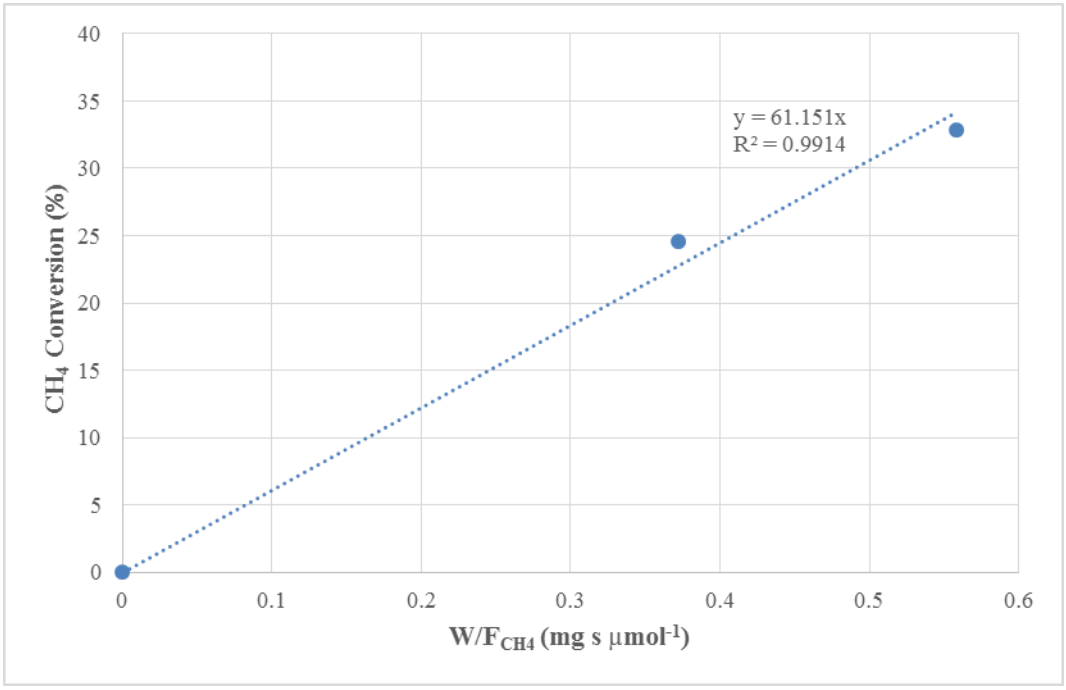

Figure A.17. Percent CH_4 conversion vs. residence time graph for Experiment 17.

REFERENCES

Ahmed, S., R. Ahluwalia, S. H. D. Lee, and S. Lottes, 2006, "A Gasoline Fuel Processor Designed to Study Quick-Start Performance", *Journal of Power Sources*, Vol. 154, pp. 214-222.

Avcı, A. K., D. L. Trimm, and Z. İ. Önsan, 2001, "Heterogeneous Reactor Modeling for Simulation of Catalytic Oxidation and Steam Reforming of Methane", *Chemical Engineering Science,* Vol. 56, pp. 641-649.

Ayabe, S., H. Omotoa, T. Utaka, R. Kikuchi, K. Sasaki, Y. Teraoka, and K. Eguchi, 2003, "Catalytic Autothermal Reforming of Methane and Propane over Supported Metal Catalysts", *Applied Catalysis A: General*, Vol. 241, pp. 261-269.

Barreto, L., A. Makihira and K. Riahi, 2003, "The Hydrogen Economy in the 21st Century: A Sustainable Development Scenario", *International Journal of Hydrogen Energy*, Vol. 28, pp. 267-284.

Budzianowski, W. M., 2010, "An Oxy-Fuel Mass-Recirculating Process for H_2 Production with CO_2 Capture by Autothermal Catalytic Oxyforming of Methane*", International Journal of Hydrogen Energy*, Vol. 35, pp. 7454-7469.

Cai, X., Y. Cai, and W. Lin, 2008, "Autothermal Reforming of Methane over Ni Catalysts Supported over ZrO_2-CeO_2-Al_2O_3", *Journal of Natural Gas Chemistry,* Vol. 17, pp. 201-207.

Çağlayan, B. S., A. K. Avcı, Z. I. Önsan, and A. E. Aksoylu, 2005, "Production of Hydrogen over Bimetallic Pt–Ni/δ-Al_2O_3: I. Indirect Partial Oxidation of Propane", *Applied Catalysis A: General,* Vol. 280, pp. 181–188.

Dantas, S. C., J. C. Escritori, R. R. Soares, and C. E. Hori, 2010, "Effect of Different Promoters on Ni/$CeZrO_2$ Catalyst for Autothermal Reforming and Partial Oxidation of Methane", *Chemical Engineering Journal*, Vol. 156, pp. 380-387.

Dantas, S. C., K.A. Resende, R.L. Rossi, A.J. Assis, and C.E. Hori, 2012, "Hydrogen Production from Oxidative Reforming of Methane on Supported Nickel Catalysts: An Experimental and Modeling Study", *Chemical Engineering Journal*, Vol. 197, pp. 407-413.

Dias, J. A. C. and J. M. Assaf, 2004, "Autothermal Reforming of Methane over Ni/γ-Al_2O_3 Catalysts: The Enhancement Effect of Small Quantities of Noble Metals", *Journal of Power Sources*, Vol. 130, pp. 106-110.

Dias, J. A. C. and J. M. Assaf, 2008, "Autothermal Reforming of Methane over Ni/γ-Al_2O_3 Promoted with Pd. The Effect of the Pd Source in Activity, Temperature Profile of Reactor and in Ignition", *Applied Catalysis A: General*, Vol. 334, pp. 243-250.

Escritori, J. C., S. C. Dantas, R. R. Soares, and C. E. Hori, 2009, "Methane Autothermal Reforming on Nickel–ceria–zirconia Based Catalysts", *Catalysis Communications*, Vol. 10, pp. 1090–1094.

Gao, J., J. Guo, D. Lianga, Z. Houa, J. Feia, and X. Zheng, 2008, "Production of Syngas via Autothermal Reforming of Methane in a Fluidized-bed Reactor over the Combined CeO_2-ZrO_2/SiO_2 Supported Ni Catalysts", *International Journal of Hydrogen Energy*, Vol. 33, pp. 5493-5500.

Gökaliler, F., B. A. Göçmen and A. E. Aksoylu, 2008, "The Effect of Ni:Pt Ratio on Oxidative Steam Reforming Performance of Pt-Ni/Al_2O_3 Catalyst", *International Journal of Hydrogen Energy*, Vol. 33, pp. 4358-4366.

Gökaliler, F., 2012, "*Characterization and Performance Analysis of Fuel Flexible OSR-WGS Catalysts",* PhD Thesis, Boğaziçi University.

Gökaliler, F., Z. I. Önsan, and A. E. Aksoylu, 2012, "Power-law Type Rate Equation for Propane ATR over Pt-Ni/Al_2O_3 Catalyst", *International Journal of Hydrogen Energy*, Vol. 37, pp. 10425-10429.

Gupta, R. B., 2009, *Hydrogen Fuel - Production, Transport, and Storage*, CRC Press, Florida.

Hagh, B. F., 2004, "Stoichiometric Analysis of Autothermal Fuel Processing", *Journal of Power Sources*, Vol. 130, pp. 85-94.

Hla, S. S., Y. Sun, G. J. Duffy, L. D. Morpeth, A. Ilyushechkin, A. Cousins, D. G. Roberts and J.H. Edwards, 2011, "Kinetics of Water-Gas Shift Reaction over a $La_{0.7}Ce_{0.2}FeO_3$ Perovskite-Like Catalyst Simulated Coal-Derived Syngas at High Temperature", *International Journal of Hydrogen Energy*, Vol. 36, pp. 518-527.

Lackner, M., W. Chen, and T. Suzuki, 2012, *Handbook of Climate Change Mitigation*, Springer, US.

Lee, S. H. D., D. V. Applegate, S. Ahmed, S. G. Calderone and T. L. Harvey, 2005, "Hydrogen from Natural Gas: Part I - Autothermal Reforming in an Integrated Fuel Processor", *International Journal of Hydrogen Energy*, Vol. 30, pp. 829-842.

Lee, I. C. and D. Chu, 2003, *Literature Review of Fuel Processing*, Army Research Laboratory.

Leppelt, R., B. Schumacher, V. Plzak, M. Kinne and R. J. Behm, 2006, "Kinetics and Mechanism of the Low-Temperature Water-Gas Shift Reaction on Au/CeO_2 Catalysts in an Idealized Reaction Atmosphere", *Journal of Catalysis*, Vol. 244, pp. 137-152.

Li, B., S. Kado, Y. Mukainakano, T. Miyazawa, T. Miyao, S. Naito, K. Okumura, K. Kunimori, and K. Tomishige, 2007, "Surface Modification of Ni Catalysts with

Trace Pt for Oxidative Steam Reforming of Methane", *Journal of Catalysis,* Vol. 245, pp. 144-155.

Li, B., X. Xu, and S. Zhang, 2013, "Synthesis Gas Production in the Combined CO_2 Reforming with Partial Oxidation of Methane over Ce-Promoted Ni/SiO_2 Catalysts", *International Journal of Hydrogen Energy*, Vol. 38, pp. 890-900.

Ma, L., D. L. Trimm, and C. Jiang, 1996, "The Design and Testing of an Autothermal Reactor for the Conversion of Light Hydrocarbons to Hydrogen: I. The Kinetics of the Catalytic Oxidation of Light Hydrocarbons", *Applied Catalysis A: General*, Vol. 138, pp. 275-283.

Malaibari, Z. O., A. Amin, E. Croiset, and W. Epling, 2014, "Performance Characteristics of Mo-Ni/Al_2O_3 Catalysts in LPG Oxidative Steam Reforming for Hydrogen Production", *International Journal of Hydrogen Energy,* Vol. 39, pp. 10061-10073.

Marino, F., C. Descorme, and D. Duprez, 2004, "Noble Metal Catalysts for the Preferential Oxidation of Carbon Monoxide in the Presence of Hydrogen", *Applied Catalysis B: Environmental,* Vol. 54, pp. 59-66.

Momirlan, M. and T. N. Veziroğlu, 2005, "The Properties of Hydrogen as a Fuel Tomorrow in Sustainable Energy System for a Cleaner Planet", *International Journal of Hydrogen Energy*, Vol. 30, pp. 795-802.

Mosayebi, Z., M. Rezaei, A. B. Ravandi, and N. Hadian, 2012, "Autothermal Reforming of Methane over Nickel Catalysts Supported on Nanocrystalline $MgAl_2O_4$ with High Surface Area", *International Journal of Hydrogen Energy*, Vol. 37, pp. 1236-1242.

Mukainakano, Y., B. Li, S. Kado, T. Miyazawa, K. Okumura, T. Miyao, S. Naito, K. Kunimori, and K. Tomishige, 2007, "Surface Modification of Ni Catalysts with Trace Pd and Rh for Oxidative Steam Reforming of Methane", *Applied Catalysis A: General*, Vol. 318, pp. 252-264.

Mukainakano, Y., K. Yoshida, S. Kadoa, K. Okumura, K. Kunimoria, and K. Tomishige, 2008a, "Catalytic Performance and Characterization of Pt–Ni Bimetallic Catalysts for Oxidative Steam Reforming of Methane", *Chemical Engineering Science,* Vol. 63, pp. 4891-4901.

Mukainakano, Y., K.Yoshida, K. Okumura, K. Kunimori, and K. Tomishige, 2008b, "Catalytic Performance and QXAFS Analysis of Ni Catalysts Modified with Pd for Oxidative Steam Reforming of Methane", *Catalysis Today,* Vol. 132, pp. 101-108.

Natesakhawat, S., X. Wang, L. Zhang and U.S. Ozkan, 2006, "Development of Chromium-free Iron-Based Catalysts for High-Temperature Water-Gas Shift Reaction", *Journal of Molecular Catalysis A: Chemical*, Vol. 260, pp. 82-94.

Nurunnabi, M., B. Li, K. Kunimori, K. Suzuki, K. Fujimoto, and K. Tomishige, 2005, "Performance of NiO-MgO Solid Solution-supported Pt Catalysts in Oxidative Steam Reforming of Methane", *Applied Catalysis A: General*, Vol. 292, pp. 272-280.

Nurunnabi, M., Y. Mukainakano, S. Kado, B. Li, K. Kunimori, K. Suzuki, K. Fujimoto, and K. Tomishige, 2006, "Additive Effect of Noble Metals on NiO-MgO Solid Solution in Oxidative Steam Reforming of Methane under Atmospheric and Pressurized Conditions", *Applied Catalysis A: General*, Vol. 299, pp. 145-156.

Razaei, M., F. Meshkani, A. B. Ravandi, B. Nematollahi, A. Ranjbar, N. Hadian, and Z. Mosayebi, 2011, "Autothermal Reforming of Methane over Ni Catalysts Supported on Nanocrystalline MgO with High Surface Area and Plated-like Shape", *International Journal of Hydrogen Energy*, Vol. 36, pp. 11712-11717.

Rowshanzamir, S., S. M. Safdarnejad, M. H. Eikani, 2012, "A CFD Model for Methane Autothermal Reforming on Ru/γ-Al_2O_3 Catalyst", *Procedia Engineering*, Vol. 42, pp. 2-24.

Ruiz, J. A. C, F. B. Passos, J. M. C. Bueno, E. F. Souza-Aguiar, L. V. Mattos and F. B. Noronha, 2008, "Syngas Production by Autothermal Reforming of Methane on Supported Platinum Catalysts", *Applied Catalysis A: General*, Vol. 334, pp. 259-267.

Shekhawat, D., D.A. Berry, T.H. Gardner, and J.J. Spivey, "*Catalytic Reforming of Liquid Hydrocarbon Fuels for Fuel Cell Applications: Catalysis Vol.19*", Royal Society of Chemistry, 2006.

Shekhawat, D., J. J. Spivey, and D. A. Berry, 2011, "*Fuel Cells: Technologies for Fuel Processing*", Elsevier, Amsterdam.

Simeone, M., L. Salemme, and C. Allouis, 2008, "Reactor Temperature Profile during Autothermal Methane Reforming on Rh/Al_2O_3 Catalyst by IR Imaging", *International Journal of Hydrogen Energy*, Vol.33, pp. 4798-4808.

Souza, M. M. V. M., and M. Schmal, 2005, "Autothermal Reforming of Methane over $Pt/ZrO_2/Al_2O_3$ Catalysts", *Applied Catalysis A: General*, Vol. 281, pp. 19-24.

Souza, M. M. V. M., N. F. P. Ribeiro, O. R. M. Neto, I. O. V. Cruz, and M. Schmal, 2007, "Autothermal Reforming of Methane over Nickel Catalysts Prepared from Hydrotalcite-Like Compounds", *Studies in Surface Science and Catalysis*, Vol. 167, pp. 451-456.

Souza, A. E. A´. M., L. J. L. Maciel, N. M. L. Filho, and C. A. M. Abreu, 2010, "Catalytic Activity Evaluation for Hydrogen Production via Autothermal Reforming of Methane", *Catalysis Today*, Vol. 149, pp. 413-417.

Takeguchi, T., S. Furukawa, M. Inoue, and K. Eguchi, 2003, "Autothermal Reforming of Methane over Ni catalysts supported over $CaO\text{-}CeO_2\text{-}ZrO_2$ Solid Solution", *Applied Catalysis A: General*, Vol. 240, pp. 223-233.

Tiemersma, T. P., A. S. Chaudhari, F. Gallucci, J. A. M. Kuipers, and M. van Sint Annaland, 2012, "Integrated Autothermal Oxidative Coupling and Steam Reforming of

Methane. Part 2: Development of a Packed Bed Membrane Reactor with a Dual Function Catalyst", *Chemical Engineering Science*, Vol. 82, pp. 232-245.

Trimm, D. L. and Z. I. Önsan, 2001, "Onboard Fuel Conversion Hydrogen-Fuel-Cell-Driven Vehicles", *Catalysis Reviews: Science and Engineering*, Vol. 43, pp. 31-84.

Wang, F., B. Qi, G. Wang, and L. Li, 2013, "Methane Steam Reforming: Kinetics and Modeling over Coating Catalyst in Micro-channel Reactor", *International Journal of Hydrogen Energy*, Vol. 38, pp. 5693-5704.

Xie, D., J. Zhao, Z. Wang, and Y. Zhang, 2013, "Syngas Production from Oxidative Methane Reforming and CO Cleaning with Water Gas Shift Reaction" *International Journal of Hydrogen Energy*, Vol. 38 pp. 10826-10832.

Xu, J. and G. F. Froment, 1989, "Methane Steam Reforming, Methanation and Water-Gas Shift: I. Intrinsic Kinetics", *AIChE Journal*, Vol. 35, pp. 88-96.

Yoshida, K., N. Begum, S. Ito, and K. Tomishige, 2009, "Oxidative Steam Reforming of Methane over Ni/α-Al_2O_3 Modified with Trace Noble Metals", *Applied Catalysis A: General*, Vol. 358, pp. 186-192.